RSC Advances

PAPER

View Article Online
View Journal | View Issue

Cite this: *RSC Adv.*, 2026, **16**, 24551

Dual inhibition of neutrophil superoxide generation and elastase release *via* JNK, ERK and FAK pathways: blockade by methoxy-chalcone derivatives

Dalia S. El-Gamil,[a] Mennatallah A. Hammam,[bc] Michael Emad,[c] Donia E. Hafez,[c] Mohamed El-Shazly,[d] Yu-Cheng Chen,[e] Yi-Hsuan Wang,[f] Po-Hsiung Kung,[ef] Michal Korinek,[g] Tsong-Long Hwang*[efhi] and Mohammad Abdel-Halim *[c]

A series of chalcone-based derivatives were synthesized and assessed for their ability to target neutrophil-driven inflammation. Strategic modifications on the 1,3-diaryl-prop-2-en-1-one scaffold, all bearing a methoxylated ring B, revealed two distinct anti-inflammatory profiles: inhibitors of both superoxide (SO) generation and elastase release, and selective SO inhibitors. Compound **17**, featuring 3-methoxy and 2,4-dichlorophenyl substitutions, demonstrated the most potent dual inhibition (IC_{50} = 1.17 μM for SO and 2.60 μM for elastase), while compound **15** selectively suppressed SO production (IC_{50} = 2.63 μM) with minimal elastase impact. Compound **17** hampered neutrophil migration without inducing cytotoxicity, and mechanistically inhibited the phosphorylation of JNK, ERK, and FAK/paxillin—key signaling pathways in neutrophil migration and activation, without altering calcium flux. These findings highlight compound **17** as a promising lead for targeting neutrophil-mediated inflammatory disorders and underscore the potential of chalcone scaffolds for precise immunomodulation.

Received 13th February 2026
Accepted 26th April 2026

DOI: 10.1039/d6ra01300g

rsc.li/rsc-advances

1 Introduction

Neutrophils are considered the first-line defenders of the immune system that respond swiftly to both infectious pathogens and non-infectious foreign invaders. Neutrophils rapidly accumulate at the site of invasion *via* complex recruitment and migration cascades where they get activated and deploy a range of potent defense mechanisms, including phagocytosis, respiratory burst, degranulation, and the formation of neutrophil extracellular traps (NETs).[1,2] The respiratory burst generates reactive oxygen species (ROS) through the NADPH oxidase complex, which actively combats pathogens. In addition, NETs, composed of myeloperoxidase, elastase, decondensed chromatin, and histones, trap and neutralize microorganisms.[3]

The intricate functional complexity of neutrophils is underscored by the diverse signaling pathways that are activated through various receptor engagements. For instance, the recruitment of neutrophils to infection sites necessitates a sophisticated interplay among neutrophils, vascular endothelial cells, and the surrounding extracellular matrix (ECM). The binding of integrins to the ECM facilitates the phosphorylation of paxillin (Pax), a cytoskeletal scaffold protein that assembles other proteins essential for the formation of the focal adhesion complex (FA).[4] Central to this complex is the focal adhesion kinase (FAK), whose autophosphorylation recruits Src protein to form an active kinase complex, that initiates downstream phosphorylation cascades that engage key signaling molecules, including mitogen-activated protein kinases (MAPKs), phosphoinositide 3-kinase (PI3K), and phospholipase C-gamma (PLCγ).[4,5] These pathways culminate in actin cytoskeleton rearrangement and the dynamic assembly and disassembly of FAs, processes that are critical for neutrophil attachment, spreading, migration, and survival.[5,6] Furthermore, FAK has been implicated in key roles in NADPH oxidase-driven

[a]*Department of Chemistry, Faculty of Pharmacy, Ahram Canadian University, Cairo, 12451, Egypt*
[b]*School of Life and Medical Sciences, University of Hertfordshire Hosted by Global Academic Foundation, New Administrative Capital, Cairo 11865, Egypt*
[c]*Department of Pharmaceutical Chemistry, Faculty of Pharmacy and Biotechnology, German University in Cairo, Cairo 11835, Egypt. E-mail: mohammad.abdel-halim@guc.edu.eg*
[d]*Department of Pharmacognosy, Faculty of Pharmacy, Ain-Shams University, Cairo, 11566, Egypt*
[e]*Center for Drug Research and Development, Graduate Institute of Healthy Industry Technology, College of Human Ecology, Chang Gung University of Science and Technology, Taoyuan 333, Taiwan. E-mail: htl@mail.cgust.edu.tw*
[f]*Graduate Institute of Natural Products, College of Medicine, Chang Gung University, Taoyuan 333, Taiwan*
[g]*Graduate Institute of Natural Products, College of Pharmacy, Kaohsiung Medical University, Kaohsiung 807, Taiwan*
[h]*Department of Anesthesiology, Chang Gung Memorial Hospital, Taoyuan 333, Taiwan*
[i]*Department of Chemical Engineering, Ming Chi University of Technology, New Taipei City 243, Taiwan*

ROS production, complement-mediated phagocytosis, and the formation of NETs in activated neutrophils.[4]

The activation of G protein-coupled receptors (GPCRs), such as the formyl peptide receptor (FPR) upon binding to the chemoattractant fMLF, is another crucial promoter of neutrophil inflammatory responses. Such receptor engagement triggers the activation of PLC and the production of inositol trisphosphate (IP3), which facilitates the mobilization and depletion of Ca^{2+} from the endoplasmic reticulum (ER) stores and promotes the influx of extracellular calcium through store-operated Ca^{2+} channels (SOCs).[7,8] The resulting surge in intracellular calcium levels significantly influences the comprehensive immune defensive machinery of neutrophils against pathogenic microorganisms.[9]

MAPKs, including p38, Jun N-terminal kinase (JNK), and extracellular signal-regulated kinase (ERK), also play a central role in modulating neutrophil-driven inflammation by regulating diverse cellular processes including chemotaxis, adhesion, migration, cytokine secretion, inflammatory gene expression, and the formation of NETs.[10–13] Furthermore, the PI3K/Akt signaling pathway is pivotal in governing critical neutrophil functions, encompassing chemotactic responses, NADPH oxidase-dependent superoxide (SO) generation, degranulation and the release of elastase, thereby enhancing the immune response.[14–16] Conversely, the cAMP/protein kinase A (PKA) pathway is thought to exert an inhibitory effect on neutrophil activation.[17]

Although essential for host defense against pathogens, the overwhelmed activation and uncontrolled immune responses by human neutrophils can lead to tissue damage and sustained inflammation implicated in various disorders, such as rheumatoid arthritis, ischemia-reperfusion injury, chronic obstructive pulmonary disease, and asthma.[2,18,19] Consequently, the modulation of neutrophil immune responses presents a promising therapeutic strategy for the management of neutrophilic inflammatory disorders.

Chalcones (1,3-diaryl-2-propen-1-ones) are well recognized as precursors to flavonoids and isoflavonoids, with their natural, semi-synthetic, and synthetic derivatives demonstrating a diverse array of pharmacological properties, including antimalarial, antimicrobial, anticancer, anti-HIV, anti-allergic, and antioxidant activities.[20] Additionally, chalcone derivatives have been found to inhibit multiple inflammatory cascades, as extensively documented in prior reviews, including those associated with neutrophil-mediated inflammation.[21,22]

Research has demonstrated that 2′,5′-dihydroxychalcone derivatives are potent inhibitors of degranulation in fMLF-stimulated rat neutrophils, evidenced by a decline in the release of β-glucuronidase and lysozyme.[23,24] The immunomodulatory properties of compound (**I**; Fig. 1) were correlated to its ability to inhibit chemotaxis, phagocytosis, and the generation of both intracellular and extracellular ROS in fMLF-activated neutrophils.[25] Moreover, compound (**II**; Fig. 1) effectively impedes the release of elastase and the synthesis of the critical chemotactic mediator and leukocyte activator leukotriene B4 (LTB4) in human neutrophils stimulated by fMLF.[26]

Hwang and colleagues have further elucidated the significant effects of chalcone derivatives (**III–V**; Fig. 1) on neutrophil functions, including respiratory burst, degranulation, adhesion, migration, and calcium mobilization, through their impact on various signaling pathways in fMLF-activated human neutrophils. Notably, (a) the inhibition of cAMP-specific phosphodiesterase (PDE) and the consequent increase in cellular cAMP levels by 3′-isopropoxychalcone (**III**),[27] (b) the selective suppression of the adhesion integrin CD11b and SOC-mediated extracellular Ca^{2+} influx by the cinnamic acid-containing bractelactone (**IV**),[28] and (c) the mitigation of intracellular alkalization and Ca^{2+} mobilization through a K^+-dependent regulatory mechanism by the heterocyclic chalcone Mannich base derivative, MVBR-28 (**V**),[17] have been highlighted as key mechanisms of anti-inflammatory action of chalcone derivatives.

The present study investigated a focused library of chalcone-based derivatives to identify novel modulators of neutrophilic inflammation. Biological screening in fMLF-activated human neutrophils revealed several compounds capable of selectively inhibiting SO production or simultaneously suppressing both SO and elastase release, all without compromising cell viability. Mechanistic studies further demonstrated that the most potent candidate exerted its anti-inflammatory and anti-migratory

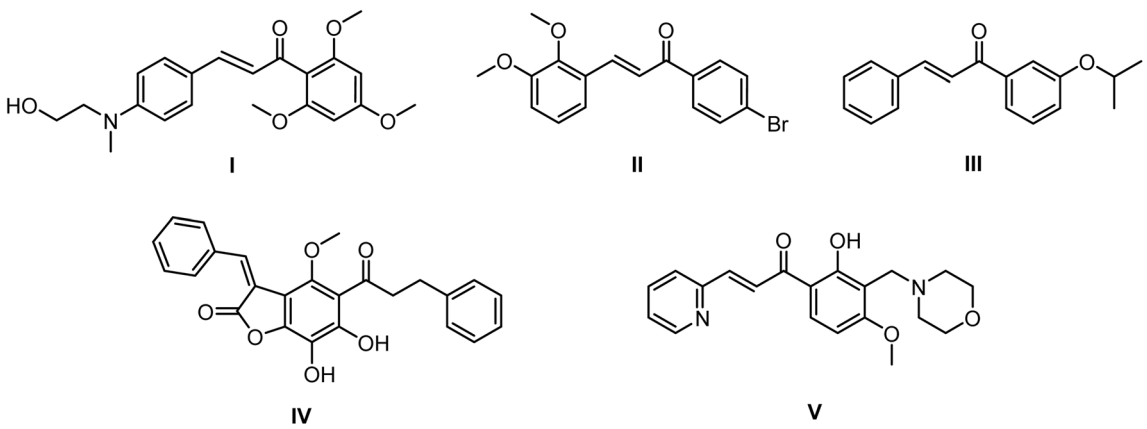

Fig. 1 Representative chalcone derivatives targeting neutrophil-mediated inflammation.

effects by specifically disrupting the JNK, ERK, and FAK/paxillin signaling pathways, highlighting its potential as a promising therapeutic lead.

2 Compound design

In a recent study, we evaluated the anti-inflammatory potential of a diverse set of 1,3-disubstituted prop-2-en-1-one derivatives in human neutrophils activated by the FPR1 agonist fMLF and cytochalasin B (CB).[29] CB serves to augment the neutrophil responses to fMLF[30] and impedes actin polymerization, allowing for a more precise analysis of the signaling pathways involved in neutrophil activation, while reducing interference from cytoskeletal changes.[31] The impact of the compounds on respiratory burst and degranulation in activated neutrophils was quantified by measuring SO anion and elastase levels, respectively. The study primarily focused on enones with electron-withdrawing substituted aryl groups at position 3, and revealed noticeable enhancement of activity when employing mono or di-methoxylated phenyl rings at position 1 (Fig. 2A).[29] Notably, compound **VI** (**6a** in ref. 29) was the most potent in suppressing both SO and elastase levels by targeting JNK and Akt signaling pathways. Meanwhile, compound **VII** (**26a** in ref. 29) inhibited SO production with minimal effects on elastase levels by modulating MAPK phosphorylation (Fig. 2A).[29]

We aimed herein to explore the anti-neutrophilic effects of a new series of chalcones (Fig. 2B), featuring electron donating methoxy group(s) on ring B, while examining the influence of various substituents on ring A. Moreover, the impact of heterocyclic surrogates for ring A, as well as the rigidification achieved by fusing ring A with the α-carbon of the enone linker, on the activity was explored.

3 Chemistry

The Claisen–Schmidt condensation reaction stands out as one of the most frequently cited synthetic methodologies in the literature for the preparation of chalcone derivatives, owing to its simplicity and the readily available starting materials. This reaction entails the condensation of an aromatic aldehyde with an appropriate ketone, catalyzed by either acidic or basic agents.[32,33] As illustrated in Scheme 1, a 10% aqueous KOH solution in methanol served as the base catalyst for this process. The targeted chalcone derivatives (**1–28**) were obtained as precipitates from the reaction mixtures in variable yields. Approximately half of the compounds reached optimal purity after simple washing with methanol/water mixtures or diethyl ether. The remaining derivatives required purification by column chromatography (CC), followed by a final diethyl ether wash. The purity of all compounds was confirmed by HPLC, and full characterization was achieved using mass spectrometry as well as ^{1}H and ^{13}C NMR spectroscopy.

4 Biological evaluation

4.1 Inhibitory effects of chalcones on superoxide anion and elastase levels in fMLF/CB stimulated human neutrophils

The synthesized chalcone derivatives (**1–28**) were assessed for their inhibitory effects on neutrophilic SO production and elastase release upon stimulation with fMLF and CB. Initial testing was conducted at a concentration of 10 μM. Compounds that demonstrated over 50% inhibition underwent further evaluation to determine their IC_{50} values. The findings shown in Table 1 support the following key SAR conclusions:

(1) The chalcone analogue featuring an unsubstituted ring A and a *para* methoxy substituted ring B (compound **1**) exhibited

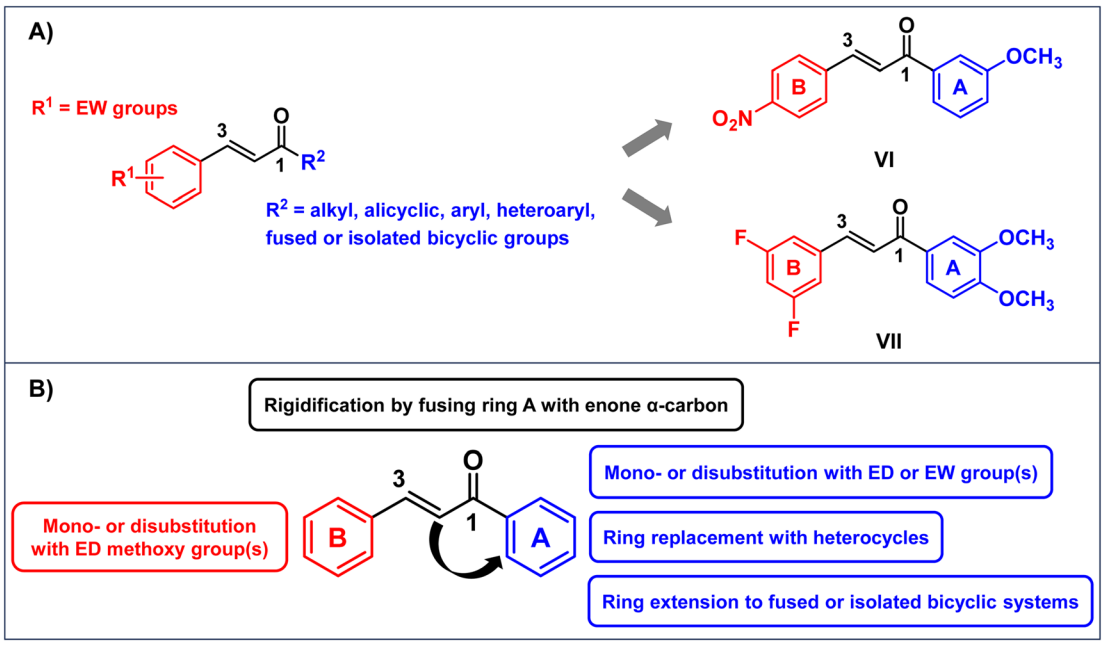

Fig. 2 (A) Chalcone derivatives with established anti-neutrophilic properties from our prior work. (B) Overview of the structural modifications introduced in the newly synthesized chalcone-based series.

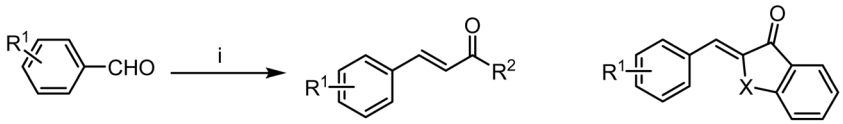

1-25 26-28

Reagents and conditions: (i) 1 equiv of the appropriate ketone in methanol, 10% KOH, 0°C then room temperature over night.

Cpd.	R^1	R^2	X	Cpd.	R^1	R^2	X
1	4-methoxy	phenyl	–	**15**	4-methoxy	2,4-dichlorophenyl	–
2	4-methoxy	2-fluorophenyl	–	**16**	4-methoxy	3,4-dichlorophenyl	–
3	4-methoxy	3-fluorophenyl	–	**17**	3-methoxy	2,4-dichlorophenyl	–
4	4-methoxy	4-fluorophenyl	–	**18**	2,4-dimethoxy	2,4-dichlorophenyl	–
5	4-methoxy	2-chlorophenyl	–	**19**	2,5-dimethoxy	2,4-dichlorophenyl	–
6	4-methoxy	3-chlorophenyl	–	**20**	3,4-dimethoxy	2,4-dichlorophenyl	–
7	4-methoxy	4-chlorophenyl	–	**21**	4-methoxy	2-thienyl	–
8	4-methoxy	2-bromophenyl	–	**22**	4-methoxy	2-pyridyl	–
9	4-methoxy	4-bromophenyl	–	**23**	4-methoxy	2-naphthyl	–
10	4-methoxy	2-hydroxyphenyl	–	**24**	4-methoxy	[1,1′-biphenyl]-4-yl	–
11	4-methoxy	3-hydroxyphenyl	–	**25**	4-methoxy	4-phenoxyphenyl	–
12	4-methoxy	4-hydroxyphenyl	–	**26**	4-methoxy	–	CH_2
13	4-methoxy	4-ethoxyphenyl	–	**27**	4-methoxy	–	CH_2-CH_2
14	4-methoxy	*p*-tolyl	–	**28**	4-methoxy	–	CH_2-O

Scheme 1 Synthesis of chalcone derivatives (**1–28**).

only marginal inhibitory effects on both fMLF-induced SO generation and elastase release. The impact of mono-substitution of ring A with various electron withdrawing halogens was subsequently investigated (compounds **2–9**). *Para* substitution with halogens generally proved detrimental to anti-neutrophilic activity. On the other hand, compounds featuring 2-chloro (**5**), 3-chloro (**6**), and 2-bromo (**8**) substitutions displayed superior efficacy compared to their fluorinated counterparts (**2** and **3**), effectively inhibiting fMLF-induced neutrophilic SO production with comparable IC_{50} values ranging from 6.26 to 7.03 μM.

(2) Ring A substitution with electron donating groups such as polar hydroxy (**10–12**) and ethoxy (**13**) groups or lipophilic methyl (**14**) generally exerted a negative impact on overall anti-neutrophilic activity. A notable exception to this trend was observed in compound **11**, which possesses a 3-hydroxy substituent and exhibited an ability to inhibit fMLF-induced SO production, resembling that of its chlorinated congener (**6**).

(3) When compared to its monochlorinated counterpart (compound **5**), 2,4-dichloro substitution of ring A (**15**) prompted a 2.7-fold enhancement in inhibitory activity against SO generation, achieving an IC_{50} value reaching 2.63 μM, while elastase release remained minimally inhibited. The substitution of ring A with 3,4-dichloro groups (compound **16**) led to diminished neutrophilic SO inhibition as compared to **15**, but successfully extended the anti-inflammatory spectrum to include the inhibition of elastase release (IC_{50} = 7.34 μM). Interestingly, maintaining the 2,4-dichloro substitution of ring A while varying ring B substitution of compound **15** with 3-methoxy (**17**), 2,5-dimethoxy (**19**), or 3,4-dimethoxy (**20**) groups granted substantially potent inhibitors of both SO generation and elastase release. Among these, compound **17** exhibited the most pronounced overall anti-neutrophilic activity, with IC_{50} values of 1.17 μM for SO generation and 2.6 μM for elastase secretion. Conversely, substituting ring B with 2,4-dimethoxy groups (in compound **18**) significantly reduced overall anti-inflammatory activity relative to compounds **17**, **19** and **20**.

(4) Substituting ring A of compound **1** with isosteric heterocycles such as 2-thienyl (**21**) and 2-pyridyl (**22**) did not yield any enhancement in anti-neutrophilic efficacy. Likewise, attempts to extend ring A into fused aromatic systems (2-naphthyl in **23**) or biaryl configurations (4-biphenyl in **24** and 4-phenoxyphenyl in **25**) did not confer any significant improvement in anti-inflammatory activity. Moreover, rigid analogues created by the fusion of ring A with the α-carbon of enone *via* methylene (**26**), ethylene (**27**), or oxymethylene (**28**) spacers demonstrated limited anti-neutrophilic potency.

At the screening concentration of 10 μM, compounds **7**, **9**, and **13** notably induced elastase release while compound **27** uniquely triggered SO anion generation in the presence of cytochalasin B alone, suggesting potential immune-modulating properties of these derivatives.

Table 1 Effects of chalcone derivatives (1–28) on levels of superoxide anion and elastase in neutrophils stimulated by fMLF and CB[a]

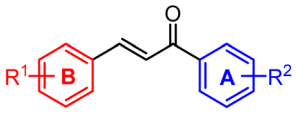

1-20, 24-25

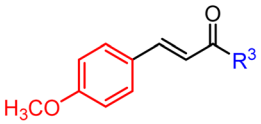

21-23

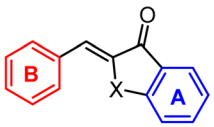

26-28

					Superoxide anion			Elastase		
Cpd.	R^1	R^2	R^3	X	Inhibition %		IC_{50}[b] (μM)	Inhibition %		IC_{50}[b] (μM)
1	4-Methoxy	H	–	–	20.04 ± 8.06		n.d.	24.45 ± 4.56	**	n.d.
2	4-Methoxy	2-Fluoro	–	–	20.13 ± 5.64	*	n.d.	2.99 ± 2.92		n.d.
3	4-Methoxy	3-Fluoro	–	–	31.12 ± 5.41	**	n.d.	14.69 ± 0.93	***	n.d.
4	4-Methoxy	4-Fluoro	–	–	28.71 ± 5.71	**	n.d.	3.31 ± 2.73		n.d.
5	**4-Methoxy**	**2-Chloro**	–	–	**57.42 ± 7.46**	***	**7.03 ± 1.22**	15.66 ± 8.52		n.d.
6	**4-Methoxy**	**3-Chloro**	–	–	**58.91 ± 3.08**	***	**6.26 ± 0.24**	27.52 ± 5.31	**	n.d.
7	4-Methoxy	4-Chloro	–	–	31.90 ± 6.96	*	n.d.	[c]		n.d.
8	**4-Methoxy**	**2-Bromo**	–	–	**59.33 ± 5.37**	***	**6.55 ± 0.33**	9.48 ± 4.36		n.d.
9	4-Methoxy	4-Bromo	–	–	33.58 ± 6.96	**	n.d.	[c]		n.d.
10	4-Methoxy	2-Hydroxy	–	–	19.46 ± 2.55	**	n.d.	21.24 ± 1.35	***	n.d.
11	**4-Methoxy**	**3-Hydroxy**	–	–	**54.74 ± 5.90**	***	**6.45 ± 0.32**	8.03 ± 2.27	*	n.d.
12	4-Methoxy	4-Hydroxy	–	–	26.93 ± 6.92	*	n.d.	13.53 ± 2.94	*	n.d.
13	4-Methoxy	4-Ethoxy	–	–	2.36 ± 0.17	***	n.d.	[c]		n.d.
14	4-Methoxy	4-Methyl	–	–	26.48 ± 5.10	**	n.d.	12.00 ± 5.83		n.d.
15	**4-Methoxy**	**2,4-Dichloro**	–	–	**79.10 ± 2.59**	***	**2.63 ± 0.15**	25.81 ± 7.96	*	n.d.
16	**4-Methoxy**	**3,4-Dichloro**	–	–	**49.38 ± 1.52**	***	**~10**	**53.27 ± 4.66**	***	**7.34 ± 2.83**
17	**3-Methoxy**	**2,4-Dichloro**	–	–	**96.30 ± 1.28**	***	**1.17 ± 0.31**	**116.78 ± 7.81**	***	**2.60 ± 0.30**
18	2,4-Dimethoxy	2,4-Dichloro	–	–	34.08 ± 8.37	*	n.d.	39.49 ± 5.41	**	n.d.
19	**2,5-Dimethoxy**	**2,4-Dichloro**	–	–	**75.88 ± 0.59**	***	**3.70 ± 0.56**	**123.91 ± 6.44**	***	**2.00 ± 0.25**
20	**3,4-Dimethoxy**	**2,4-Dichloro**	–	–	**80.28 ± 2.88**	***	**2.54 ± 0.61**	**63.68 ± 3.40**	***	**6.35 ± 0.32**
21	–	–	2-Thienyl	–	28.83 ± 8.45	*	n.d.	31.70 ± 8.96	*	n.d.
22	–	–	2-Pyridyl	–	5.52 ± 4.12		n.d.	17.34 ± 5.29	*	n.d.
23	–	–	2-Naphthyl	–	29.19 ± 9.4	*	n.d.	42.87 ± 4.93	**	n.d.
24	4-Methoxy	4-Phenyl	–	–	4.81 ± 4.17		n.d.	18.86 ± 5.46	*	n.d.
25	4-Methoxy	4-Phenoxy	–	–	2.47 ± 2.84		n.d.	23.49 ± 3.54	**	n.d.
26	–	–	–	CH_2	9.09 ± 0.23	***	n.d.	14.84 ± 3.57	*	n.d.
27	–	–	–	CH_2–CH_2	[c]		n.d.	8.69 ± 3.25		n.d.
28	–	–	–	CH_2–O	36.95 ± 4.85	**	n.d.	17.34 ± 3.82	*	n.d.
LY294002[d]					101.58 ± 2.64	***	2.02 ± 0.84	82.53 ± 3.76	***	4.93 ± 2.48

[a] Inhibition percentages (inhibition %) are assessed at 10 μM concentration. Results are provided as mean ± S.E.M. (n = 3–5); n.d. not determined. *p < 0.05, **p < 0.01, ***p < 0.001 in comparison to the control (fMLF/CB). [b] Half-maximal inhibitory concentration (IC_{50}). [c] When pretreated with cytochalasin B alone, 10 μM of compound **27** raised the neutrophilic levels of superoxide anion while compounds **7**, **9** and **13** induced elastase release. [d] Positive control.

Fig. 3 summarizes the SAR findings, delineating two distinct neutrophil-targeting anti-inflammatory profiles among the examined chalcone derivatives. One profile embraces dual suppressors of neutrophilic SO and elastase levels (highlighted in green), with compound **17** emerging as the most potent. The other profile comprises exclusive inhibitors of SO anion production (highlighted in yellow), with compound **15** exhibiting the highest potency. Notably, no compounds were identified that selectively inhibited elastase release without concurrently affecting SO production.

4.2 Cytotoxicity evaluation of lead chalcone derivatives in human neutrophils

Lactate dehydrogenase (LDH), an enzyme typically confined within the intracellular milieu, is known to be liberated into the extracellular space upon compromise of the plasma membrane integrity due to cellular injury or lysis.[34] Consequently, in studies assessing neutrophil viability, quantifying LDH present in the supernatant serves as a credible marker for cell membrane disruption and subsequently cytotoxicity.[35]

In this context, we have further explored the potential cytotoxic effects of the four potent anti-neutrophilic chalcone derivatives (**16**, **17**, **19**, **20**), identified for their inhibitory impact on both fMLF-induced SO production and elastase release. Neutrophils were treated with 10 μM concentrations of these compounds, and the resultant LDH levels were measured and compared to those in untreated controls (0.1% DMSO). The results shown in Table 2 indicate preserved cell membrane integrity and negligible cytotoxicity, thereby reinforcing the potential of these chalcone analogues as promising therapeutic agents targeting neutrophil-mediated inflammatory responses.

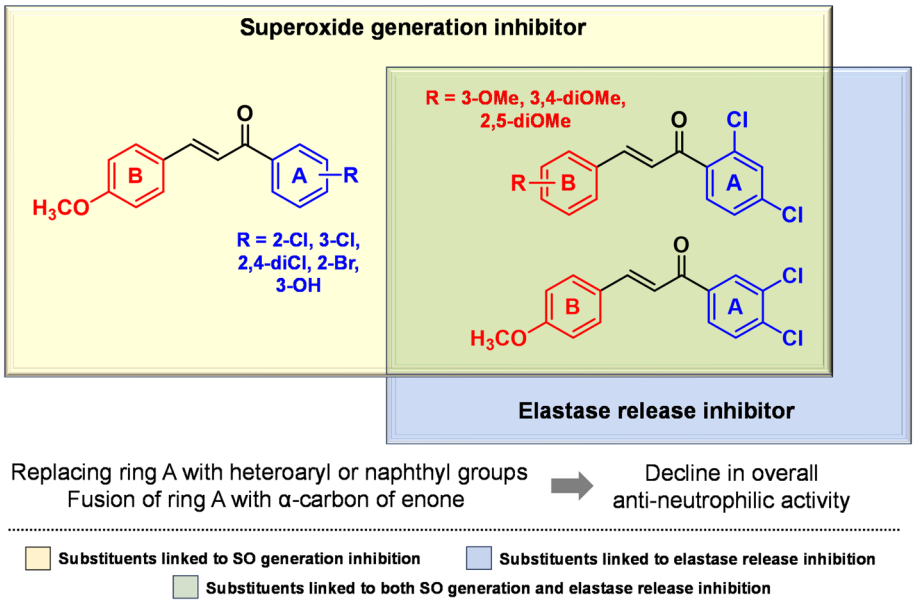

Fig. 3 Summary of SAR findings highlighting key structural features associated with anti-neutrophilic activity. Substituents linked to superoxide inhibition are marked in yellow, those associated with elastase inhibition in blue, and dual-action features are indicated at the intersection in green.

Table 2 Impact of potent chalcone derivatives on human neutrophil viability

Cpd.	Cell viability[a] (%)
16	93.01 ± 2.29
17	96.03 ± 3.39
19	99.87 ± 0.86
20	92.40 ± 2.91

[a] Percentage of cell viability (%) at 10 μM. Results are presented as mean ± S.E.M. (n = 4–5).

4.3 Extended functional and mechanistic profiling of compound 17

Given its superior dual inhibitory activity against both SO generation and elastase release, compound **17** was selected for further biological characterization. To gain deeper insights into its potential as a modulator of neutrophil-driven inflammation, additional functional assays were conducted, including evaluation of its effects on neutrophil chemotaxis and analysis of key downstream signaling pathways involved in neutrophil activation.

4.3.1 Compound 17 attenuates fMLF-induced neutrophil migration. As delineated in the introduction, numerous studies have elucidated the precise mechanisms through which chalcone derivatives modulate neutrophil migration and chemotaxis, thereby presenting promising avenues for anti-inflammatory therapies.[20,22,25]

To evaluate the impact of compound **17** on neutrophil migration in response to the chemoattractant fMLF, a microchemotaxis chamber was employed. This apparatus comprises two compartments: the upper chamber, containing neutrophils pretreated with either DMSO (serving as the control) or **17** (10 μM), and the lower chamber, infused with or without 0.1 μM fMLF. These compartments are separated by a microporous membrane that facilitates cellular migration while averting fluid intermixing. This configuration establishes a stable concentration gradient, directing neutrophils from the upper to the lower chamber.

Flow cytometry was utilized to quantify the migrating neutrophils, thus providing insights into their chemotactic activity. As depicted in Fig. 4, compound **17** prompted an approximate 80% reduction in the migratory capacity of neutrophils in response to fMLF, suggesting potential therapeutic benefits in mitigating excessive neutrophil-driven inflammatory responses.

4.3.2 Compound 17 disrupts JNK and ERK phosphorylation in fMLF-induced human neutrophils. The MAPKs (p38, JNK, and ERK) and PI3K/Akt signaling pathways are critically implicated in the modulation of neutrophil-mediated inflammatory responses. These cascades orchestrate essential cellular processes, including chemotaxis, adhesion, aggregation, and transmigration across endothelial barriers, all of which are crucial for the effective recruitment of neutrophils to sites of infection or tissue damage. Furthermore, these kinases are integral for the production of pro-inflammatory cytokines, thus perpetuating the inflammatory response.[11–13,15]

The activation of the PI3K/Akt pathway in neutrophils has been demonstrated to induce key activation processes, including oxidative burst and degranulation.[14–16] Moreover, MAPKs are involved in regulating the lifespan of neutrophils by influencing apoptotic pathways, ensuring the timely clearance of these cells following the resolution of infection.[36] ERK activation, often initiated through immune receptors, promotes the

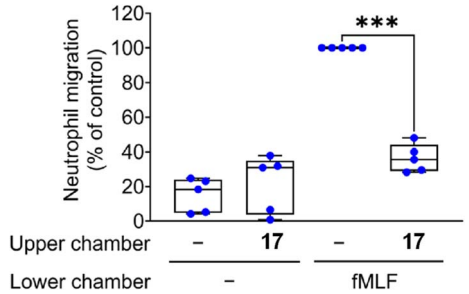

Fig. 4 Compound **17** suppresses neutrophil chemotaxis. Neutrophils treated with DMSO (0.1%) or **17** (10 μM) were placed in the upper chamber of the chemotaxis wells. fMLF (0.1 μM) was added to the lower chamber to induce neutrophil migration for 90 min ($n = 5$). Results are presented as box-and-whiskers plots with median (min to max) ***$p < 0.001$ compared with fMLF control.

expression of inflammatory genes, thereby enhancing the effector functions of neutrophils.[12,37] Intriguingly, ERK activation has also been observed to occur independently of mitogen-activated protein kinase (MEK), affecting gene expression and neutrophil behavior through non-canonical mechanisms.[38] Furthermore, JNK signaling was proven essential for neutrophil responses to bacterial infections, including the formation of NETs through a process known as suicidal NETosis.[39,40]

Previous investigations have established a correlation between the capacity of chalcone derivatives (**VI** and **VII**; Fig. 1) to inhibit respiratory burst and degranulation and their ability to impede MAPK and/or Akt phosphorylation.[29] Compound **17** has been identified as the most potent inhibitor within the present series, effectively attenuating fMLF-induced SO and elastase secretion, in addition to significantly suppressing neutrophil migration in response to fMLF. Consequently, the current study sought to elucidate whether these anti-neutrophilic properties of **17** are mediated through modulation of the MAPK or PI3K/Akt signaling cascades.

Immunoblotting analyses revealed that treatment of human neutrophils with 0.1 μM of the FPR1 agonist fMLF resulted in elevated phosphorylation levels of MAPKs (JNK, ERK, and p38) and Akt. Conversely, treatment with **17** (10 μM) significantly attenuated the phosphorylation of JNK and ERK in neutrophils stimulated by fMLF, while the phosphorylation states of p38 and Akt remained unaffected (Fig. 5). These findings suggest that **17** exerts its inhibitory effects on fMLF-induced oxidative burst, degranulation, and migration partly through the suppression of JNK and ERK phosphorylation, highlighting its potential as a targeted modulator of neutrophilic inflammatory responses.

4.3.3 Compound 17 impairs FAK/paxillin phosphorylation in activated neutrophils. Paxillin is a pivotal cytoskeletal protein that is actively recruited to sites of integrin-extracellular matrix adhesion. Upon phosphorylation, paxillin generates binding sites necessary for the assembly of key focal adhesion proteins such as talin, vinculin, tensin, and FAK. The autophosphorylation of FAK at Tyr397 following integrin activation establishes a binding site for the Src homology 2 (SH2) domain of Src tyrosine kinases. This recruitment facilitates the formation of an active FAK/Src kinase complex, which subsequently phosphorylates additional sites on FAK (such as Tyr576 and Tyr925), thereby activating multiple signaling pathways and growth factor signals that regulate cellular processes such as spreading, migration, and survival. Simultaneously, phosphorylation of paxillin by Src at tyrosine residues 88 and 118, along with FAK-induced phosphorylation at Tyr118 and Tyr31, leads to paxillin's dissociation from adhesion complexes, enhancing neutrophil transmigration across endothelial cells.[5,6,41,42]

Beyond its involvement in neutrophil transmigration, FAK is pivotal in NADPH oxidase-mediated respiratory burst and complement-mediated phagocytosis in integrin-adherent neutrophils.[4] Additionally, FAK contributes to fMLF-induced SO production in suspended neutrophils, indicating FAK regulation *via* GPCRs independently of integrins.[4] FAK also influences NET formation, where FAK inhibition diminishes NET production and cytokine release likely due to impaired PI3K phosphorylation.[43] Moreover, neutrophils with down-regulated or knocked-out FAK were found to display compromised pathogen-killing abilities and lower survival rates.[4]

The chalcone derivative flavokawain C has been previously documented to inhibit the FAK/PI3K/Akt signaling pathway, suppressing the proliferation and migration of liver cancer cells.[44] Another flavone chalcone derivative has also demonstrated the capacity to impede the invasion and migration of gastric cancer cells by inhibiting FAK and JNK1/2 phosphorylation, which subsequently downregulates matrix metalloproteinases.[45]

Motivated by these findings and having confirmed compound **17**'s ability to suppress respiratory burst and migration in fMLF-stimulated neutrophils, we embarked on an investigation to determine whether the observed anti-neutrophilic effects could be attributed to the inhibition of FAK or paxillin signaling. Neutrophils stimulated with 0.1 μM fMLF were incubated with 10 μM of **17**, and the levels of phosphorylated FAK at tyrosine residues 397, 576, and 925, as well as phosphorylated paxillin at tyrosine residues 31 and 118, were semi-quantified relative to their respective unphosphorylated forms using western blot analysis. The results revealed a significant inhibition of tyrosine phosphorylation for both FAK and paxillin at all examined sites (Fig. 6), thereby underscoring the inhibition of FAK/paxillin signaling as a key contributor to the compound's observed anti-inflammatory efficacy.

4.3.4 Compound 17 exerts anti-inflammatory effects independent of calcium signaling. The activation of G protein-coupled receptors and tyrosine kinase-coupled receptors on neutrophils initiates the PLC/IP3 signaling cascade. Upon binding to its receptors on the endoplasmic reticulum, IP3 induces the release of stored calcium, which subsequently triggers the influx of extracellular Ca^{2+} through the gradual activation of store-operated calcium channels. The mobilization of Ca^{2+} and the precise regulation of intracellular Ca^{2+} concentrations are crucial for controlling the full spectrum of pro-inflammatory responses in neutrophils.[7,9] Specifically, fMLF-induced Ca^{2+} mobilization is essential for the complete activation of NADPH oxidase, the respiratory burst, and

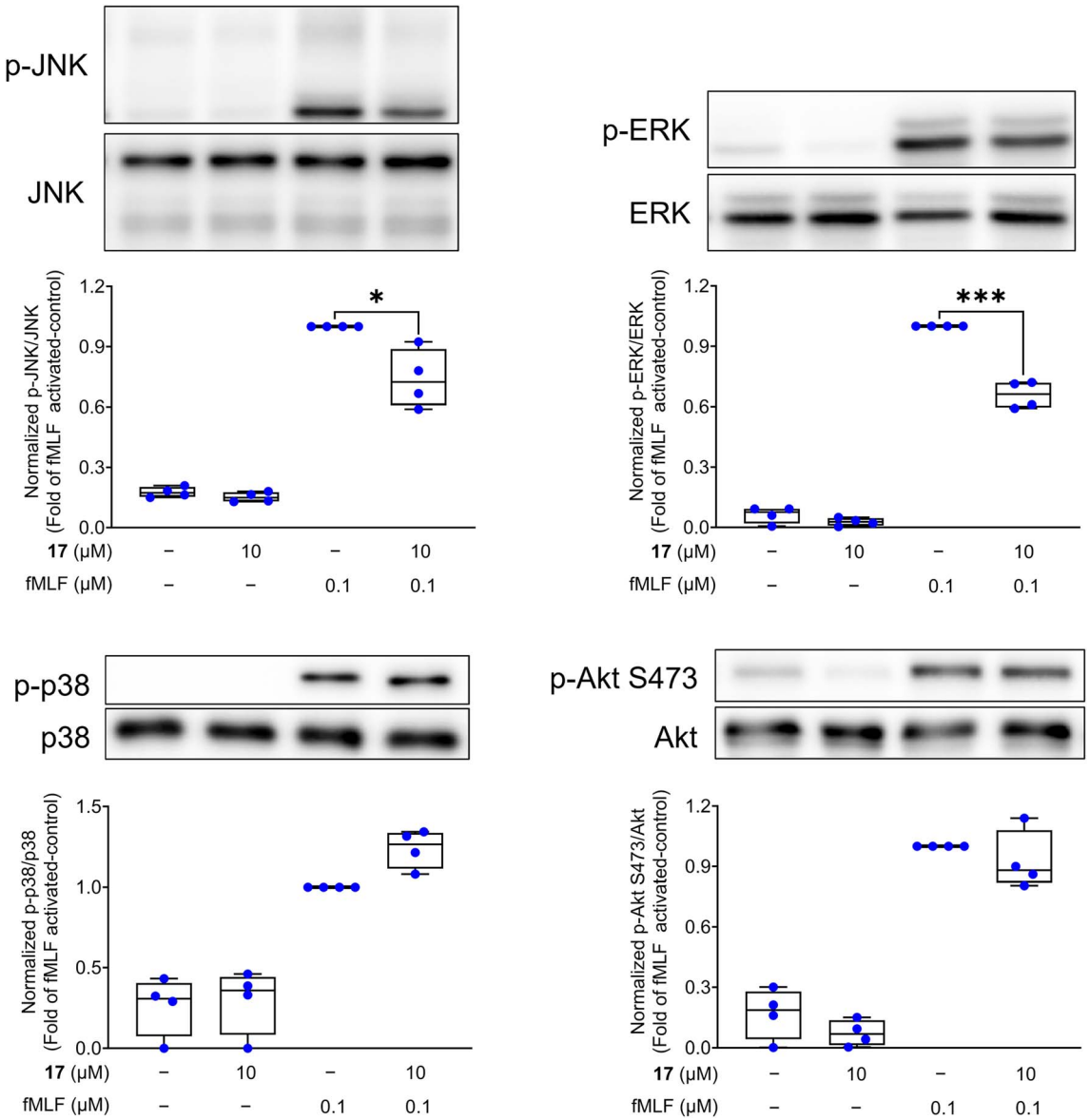

Fig. 5 Compound **17** attenuates the phosphorylation of JNK and ERK in fMLF-stimulated neutrophils. Human neutrophils were pretreated with either 0.1% DMSO or 10 μM of compound **17** for 5 minutes, followed by exposure to 0.1 μM fMLF for 30 seconds or left unstimulated. After treatment, cells were lysed and analyzed *via* immunoblotting, where the phosphorylation levels of (A) JNK, (B) ERK, (C) p38 MAPK, and (D) Akt were determined using antibodies specific to both the phosphorylated and total forms of each protein. Phosphorylation data were normalized to the corresponding total protein levels and expressed as mean ± S.E.M. Statistical significance was determined relative to the DMSO + fMLF group (*$p < 0.05$, ***$p < 0.001$; $n = 3$).

degranulation processes in human neutrophils.[46] Additionally, β2-integrin activation, cytoskeletal reorganization, and neutrophil migration within tissues are all governed by Ca^{2+} signaling.[46] It has been proposed that an elevation in intracellular Ca^{2+} concentration ($[Ca^{2+}]_i$) during Fc receptor-mediated phagocytosis is necessary for the early trafficking of azurophilic granules to the phagosome prior to its sealing.[47] Furthermore, an increase in $[Ca^{2+}]_i$ activates calcineurin, which dephosphorylates NFAT, allowing its translocation to the nucleus where it becomes transcriptionally active, promoting the expression of cytokines.[9] A localized rise in intracellular $[Ca^{2+}]$ also facilitates the vesicular transport of NETs to the plasma membrane, promoting their secretion into the extracellular space without compromising membrane integrity.[48]

Bractelactone (**IV**; Fig. 1) demonstrated a potent capacity to suppress SO anion generation, elastase release, as well as the adhesion and migration of fMLF-stimulated human neutrophils. These effects were achieved through the selective inhibition of store-operated calcium entry, without inducing any alterations in MAPKs or Akt phosphorylation, or modulating cAMP levels.[28] Moreover, the anti-inflammatory properties of MVBR-28 (**V**; Fig. 1) were partially attributed to potassium-mediated regulation of calcium mobilization, operating independently of the FPR1 receptor or the cAMP/PKA signaling

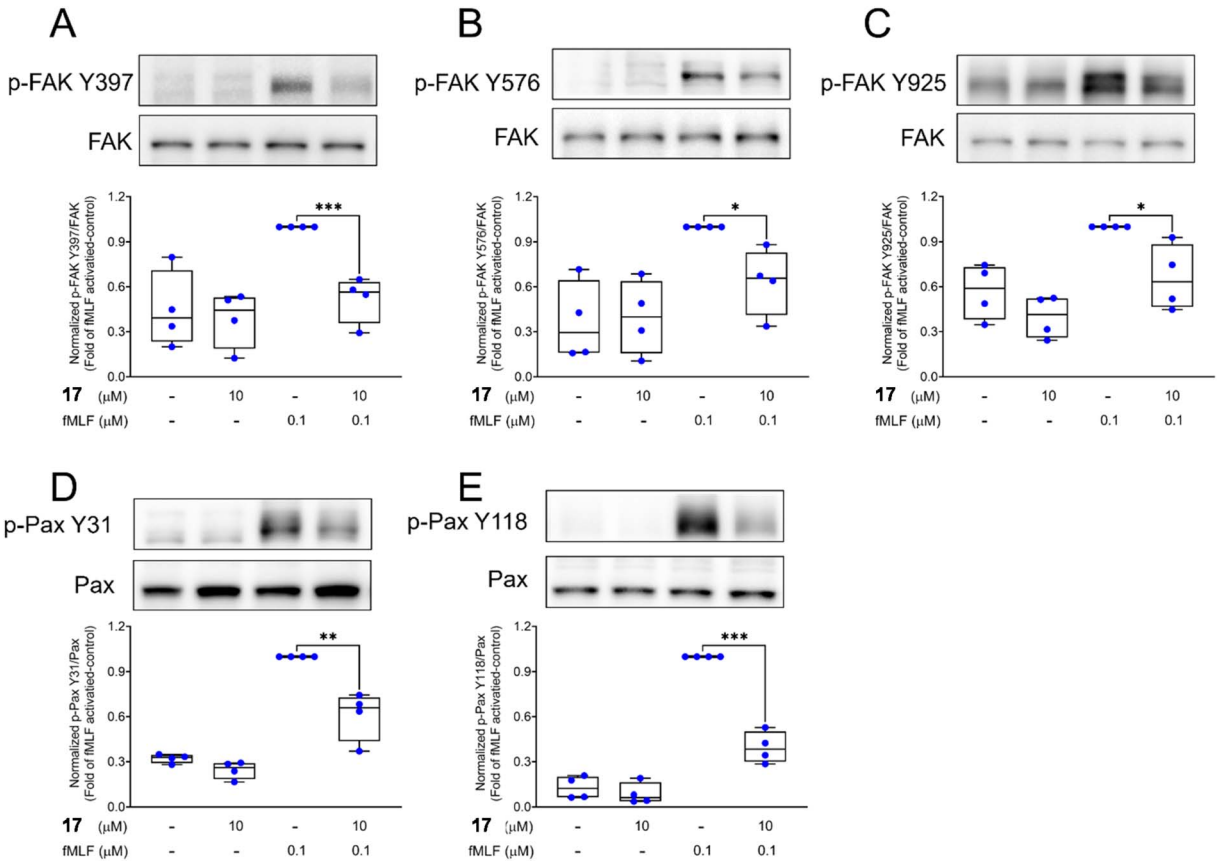

Fig. 6 Compound **17** suppresses focal adhesion kinase (FAK) and paxillin (Pax) phosphorylation in fMLF-stimulated human neutrophils. Neutrophils were pre-incubated with either 0.1% DMSO (control) or compound **17** (10 μM) for 5 minutes, followed by stimulation with fMLF (0.1 μM) for 30 seconds. Phosphorylation levels of FAK at Tyr397 (A), Tyr576 (B), and Tyr925 (C), as well as paxillin at Tyr31 (D) and Tyr118 (E), were assessed by immunoblotting using phospho-specific antibodies. Data were normalized to the fMLF-stimulated control group and are presented as mean ± S.E.M. ($n = 4$). *$p < 0.05$, **$p < 0.01$, ***$p < 0.001$ *versus* fMLF control.

pathway.[17] These observations underscore the critical role of calcium signaling in neutrophil functionality, prompting further investigation into the potential influence of compound **17** on calcium mobilization. As illustrated in Fig. 7, the $[Ca^{2+}]_i$ was rapidly elevated in neutrophils following fMLF (0.1 μM) stimulation, whereas **17** did not exhibit any inhibitory effect on calcium mobilization. Consequently, it can be inferred that the anti-inflammatory actions of **17** are not mediated through calcium signaling pathways.

Fig. 8 summarizes the key intracellular targets and downstream inflammatory processes modulated by compound **17** in fMLF-activated neutrophils.

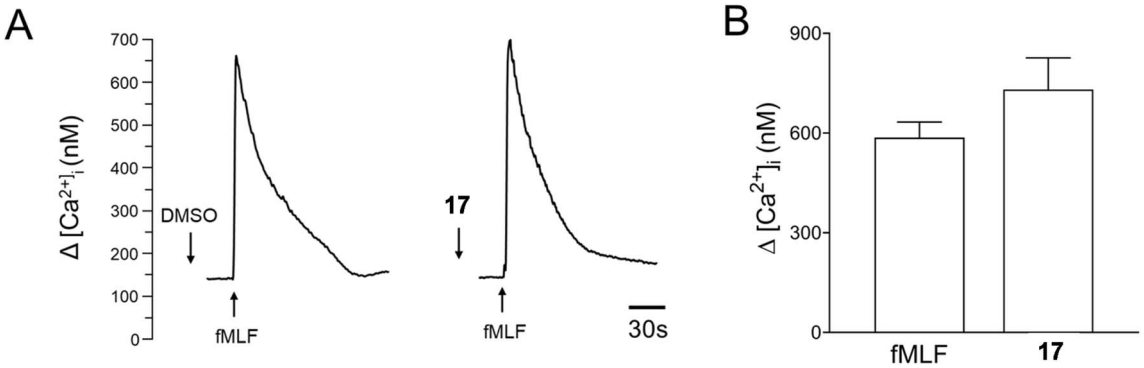

Fig. 7 Compound **17** does not alter Ca^{2+} mobilization in fMLF-induced human neutrophils. (A) Fluo-4-labeled neutrophils were treated with DMSO or **17** (10 μM) for 5 min before activating with fMLF (10 μM). Ca^{2+} mobilization was determined by a spectrofluorometer. (B) The $\Delta[Ca^{2+}]_i$ of (A) was calculated. Data are shown as means ± SEM ($n = 5$).

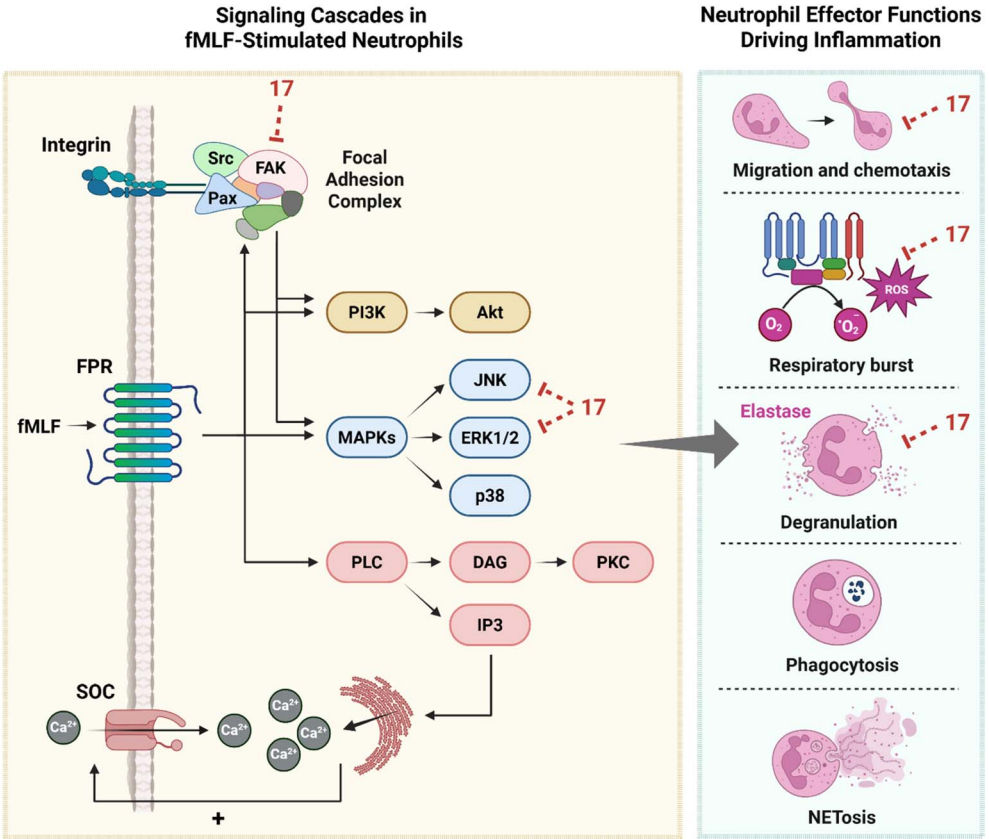

Fig. 8 Mechanistic overview of compound **17** as a selective modulator of fMLF-induced neutrophil inflammatory responses. fMLF engagement with FPR triggers multiple intracellular signaling pathways, including MAPKs (ERK1/2, JNK, p38), PI3K/Akt, PLC/PKC, and integrin-associated FAK/paxillin signaling in addition to PLC/IP3-mediated calcium mobilization from ER stores and subsequent store-operated calcium entry. These cascades regulate key effector functions—chemotaxis, respiratory burst, and degranulation. Compound **17** selectively inhibits ERK1/2, JNK, and FAK/paxillin phosphorylation, leading to suppression of SO production, elastase release, and migration, while sparing PI3K/Akt signaling and calcium mobilization. Created in BioRender. Hwang, T. (2026) https://BioRender.com/nvr2r91.

5 Conclusion

In the current study, a novel series of chalcone derivatives based on the 1,3-diaryl-prop-2-en-1-one scaffold was synthesized and evaluated for their modulatory effects on fMLF-induced neutrophil activation. Structure–activity relationship analysis revealed that the combination of electron-donating methoxy groups on ring B and electron-withdrawing 2,4-dichloro substituents on ring A was critical in defining two distinct pharmacological profiles: dual inhibitors of SO generation and elastase release, and selective inhibitors of SO generation alone. Throughout the investigated series, no compounds were found to inhibit elastase release exclusively without affecting SO generation.

Among the synthesized compounds, compound **17** emerged as the most potent dual inhibitor, displaying IC_{50} values of 1.17 μM for SO production and 2.60 μM for elastase release, while maintaining excellent safety with negligible cytotoxicity and robust inhibition of neutrophil chemotaxis. In contrast, compound **15** selectively inhibited SO generation ($IC_{50} = 2.63$ μM) with minimal effect on elastase release, highlighting its potential as a more targeted modulator of oxidative neutrophil responses.

Mechanistic investigations demonstrated that the anti-inflammatory effects of compound **17** are partly mediated through selective attenuation of ERK and JNK phosphorylation, without significant modulation of p38 or Akt pathways. Furthermore, **17** effectively suppressed phosphorylation of FAK and paxillin—key components of the integrin-associated signaling cascade—suggesting that disruption of this axis underlies its inhibition of neutrophil migration and respiratory burst. Notably, **17** did not interfere with intracellular calcium mobilization, suggesting a mechanism of action independent of store-operated calcium entry pathways.

Altogether, the dual inhibition profile, potent activity, and favorable safety of compound **17** position it as a highly promising lead for the development of therapeutic agents targeting neutrophil-driven inflammatory disorders. While the present findings establish a solid foundation at the cellular level, several important avenues remain to be explored in future studies. First, although compound **17** was shown to inhibit the phosphorylation of JNK, ERK, and FAK/paxillin, the direct molecular target to which it initially binds has not yet been identified. Future work employing target identification strategies will be essential to delineate the precise binding partner(s) and fully

characterize the pharmacological mechanism of action. Second, broader toxicity profiling, including evaluation against additional cell types such as hepatocytes, as well as assessment of genotoxicity, will be necessary to build a more comprehensive safety profile. Third, the present findings are derived entirely from *in vitro* assays using isolated human neutrophils, which, while informative at the cellular level, do not recapitulate the complexity of systemic inflammatory responses. Validation of the anti-inflammatory efficacy of compound **17** in appropriate *in vivo* animal models of neutrophil-driven inflammatory disorders, alongside evaluation of its pharmacokinetic properties and systemic bioavailability, will be critical to have a comprehensive overview over its pharmacological profile.

6 Experimental section

6.1 Chemistry

Solvents and reagents were obtained from commercial sources and used as received. The purity of all tested compounds was confirmed by UHPLC linked to mass spectrometry, with a purity level of at least 95%. The structure of all derivatives was determined *via* ^{1}H and ^{13}C NMR spectra that were recorded on a Varian Mercury 400 spectrometer, using the residual protonated $CDCl_3$ or DMSO-d_6 signals as the reference for chemical shifts. Ultra-high-performance liquid chromatography coupled with electrospray ionization tandem mass spectrometry (UHPLC-ESI-MS/MS) was conducted using a Waters ACQUITY Xevo TQD platform. The system comprised an ACQUITY UPLC H-Class module interfaced with a Xevo™ TQD triple-quadrupole mass spectrometer equipped with an electrospray ion source (Waters Corporation, Milford, MA, USA). Chromatographic separation was achieved on an ACQUITY BEH C18 column (100 × 2.1 mm, 1.7 μm particle size; Waters, Ireland). The mobile phase comprised 0.1% trifluoroacetic acid (TFA) in water (solvent A) and 0.1% TFA in acetonitrile (solvent B). The UHPLC gradient elution protocol operated at a flow rate of 200 μL min^{-1}, initiating with 5% solvent B held constant for 0.5 min, followed by a linear ramp to 100% B over 3 min, an isocratic hold at 100% B for 2 min, a return to 5% B within 2 min, and re-equilibration at 5% B for 0.5 min. Mass spectrometric detection parameters included a capillary voltage of 3.5 kV, cone voltage of 20 V, RF lens voltage of 2.5 V, source temperature of 150 °C, and desolvation gas temperature of 500 °C. Nitrogen served as both desolvation gas (1000 L h^{-1}) and cone gas (20 L h^{-1}). Instrument control, data acquisition, and processing were performed using MassLynx™ software version 4.1 (Waters). Melting points were measured using a Buchi B-540 melting point apparatus and are presented without correction.

6.1.1 General procedure for enone synthesis. A solution containing 10 mmol of the designated ketone in 50 mL of methanol was cooled using an ice bath, followed by the addition of 30 mL of 10% aqueous KOH. Subsequently, 10 mmol of the specified aromatic aldehyde was added slowly. The mixture was left to stir at room temperature overnight. The resulting precipitate was filtered and washed three times with either a 5 : 3 methanol/water mixture or diethyl ether.[49] In several cases, further purification by CC followed by a final diethyl ether wash was required to attain optimal purity.

*6.1.1.1 (E)-3-(4-Methoxyphenyl)-1-phenylprop-2-en-1-one (**1**).* *p*-Methoxybenzaldehyde and acetophenone were used as reactants; the resulting precipitate was purified by CC (EtOAc : hexane 1 : 4) followed by washing with diethyl ether (3 × 10 mL) to give the desired pure product as a white solid (79% yield); mp 75–77 °C (as reported in ref. 50); ^{1}H NMR (400 MHz, $CDCl_3$) δ 7.88 (d, J = 7.6 Hz, 2H), 7.66 (d, J = 15.6 Hz, 1H), 7.45 (dd, J = 15.7, 7.7 Hz, 3H), 7.36 (t, J = 7.5 Hz, 2H), 7.28 (d, J = 15.6 Hz, 1H), 6.80 (d, J = 8.3 Hz, 2H), 3.72 (s, 3H); ^{13}C NMR (101 MHz, $CDCl_3$) δ 191.01, 162.13, 145.13, 138.95, 132.99, 130.67, 129.00, 128.85, 128.06, 120.23, 114.86, 55.84; MS (ESI): m/z = 239.5 (M + H)$^+$.

*6.1.1.2 (E)-1-(2-Fluorophenyl)-3-(4-methoxyphenyl)prop-2-en-1-one (**2**).* *p*-Methoxybenzaldehyde and 2′-fluoroacetophenone were used as reactants; the resulting precipitate was purified by CC (EtOAc : hexane 1 : 4) followed by washing with diethyl ether (3 × 10 mL) to give the desired pure product as a yellow solid (80% yield); mp 54–56 °C (as reported in ref. 51); ^{1}H NMR (400 MHz, $CDCl_3$) δ 7.71 (t, J = 1.9 Hz, 1H), 7.63 (d, J = 15.7 Hz, 1H), 7.49 (d, J = 8.4 Hz, 2H), 7.43 (td, J = 7.7, 5.1 Hz, 1H), 7.24–7.13 (m, 2H), 7.07 (dd, J = 10.8, 8.2 Hz, 1H), 6.84 (d, J = 8.3 Hz, 2H), 3.77 (s, 3H); ^{13}C NMR (101 MHz, $CDCl_3$) δ 189.28 (d, J = 2.6 Hz), 161.97, 161.47 (d, J = 242.6 Hz), 144.99, 133.74 (d, J = 8.8 Hz), 131.05 (d, J = 2.9 Hz), 130.55, 129.12, 127.56, 124.58 (d, J = 3.4 Hz), 123.58 (d, J = 6.4 Hz), 116.61 (d, J = 23.1 Hz), 114.57, 55.55; MS (ESI): m/z = 257.3 (M + H)$^+$.

*6.1.1.3 (E)-1-(3-Fluorophenyl)-3-(4-methoxyphenyl)prop-2-en-1-one (**3**).* *p*-Methoxybenzaldehyde and 3′-fluoroacetophenone were used as reactants;[50] The resulting precipitate was purified by CC (EtOAc : hexane 1 : 4) followed by washing with diethyl ether (3 × 10 mL) to give the desired pure product as a yellow semisolid (77% yield); ^{1}H NMR (400 MHz, $CDCl_3$) δ 7.74–7.68 (m, 2H), 7.60 (d, J = 2.6 Hz, 1H), 7.52 (d, J = 8.3 Hz, 2H), 7.38 (td, J = 8.0, 5.4 Hz, 1H), 7.26 (d, J = 15.6 Hz, 1H), 7.18 (t, J = 4.2 Hz, 1H), 6.85 (d, J = 8.3 Hz, 2H), 3.77 (s, 3H); ^{13}C NMR (101 MHz, $CDCl_3$) δ 189.27 (d, J = 2.2 Hz), 162.68 (d, J = 248.0 Hz), 162.04, 145.58, 140.81 (d, J = 6.3 Hz), 130.51, 130.33 (d, J = 7.7 Hz), 127.53, 124.20 (d, J = 3.0 Hz), 119.65 (d, J = 21.5 Hz), 119.33, 115.35 (d, J = 22.3 Hz), 114.62, 55.57; MS (ESI): m/z = 257.2 (M + H)$^+$.

*6.1.1.4 (E)-1-(4-Fluorophenyl)-3-(4-methoxyphenyl)prop-2-en-1-one (**4**).* *p*-Methoxybenzaldehyde and 4′-fluoroacetophenone were used as reactants; the resulting precipitate was collected by filtration and washed using (3 × 10 mL) of 5 : 3 mixture of methanol and water to give the desired pure product as a yellowish white solid (74% yield); mp 83–84.5 °C (as reported in ref. 50); ^{1}H NMR (400 MHz, DMSO-d_6) δ 8.25–8.20 (m, 2H), 7.86–7.69 (m, 4H), 7.37 (t, J = 8.6 Hz, 2H), 7.01 (d, J = 8.2 Hz, 2H), 3.81 (s, 3H); ^{13}C NMR (101 MHz, DMSO-d_6) δ 187.54, 164.94 (d, J = 251.5 Hz), 161.44, 144.20, 134.48 (d, J = 2.8 Hz), 131.36 (d, J = 9.4 Hz), 130.87, 127.27, 119.27, 115.70 (d, J = 21.7 Hz), 114.41, 55.38; MS (ESI): m/z = 257.3 (M + H)$^+$.

*6.1.1.5 (E)-1-(2-Chlorophenyl)-3-(4-methoxyphenyl)prop-2-en-1-one (**5**).* *p*-Methoxybenzaldehyde and 2′-chloroacetophenone were used as reactants; the resulting precipitate was purified by CC (EtOAc : hexane 2 : 3) followed by washing with diethyl ether

(3 × 10 mL) to give the desired pure product as an off-white solid (78% yield); mp 78–80 °C (as reported in ref. 50); ^{1}H NMR (400 MHz, $CDCl_3$) δ 7.51 (d, J = 8.3 Hz, 2H), 7.46–7.32 (m, 5H), 6.99 (d, J = 16.2 Hz, 1H), 6.91 (d, J = 8.3 Hz, 2H), 3.84 (s, 3H); ^{13}C NMR (101 MHz, $CDCl_3$) δ 194.36, 162.42, 146.81, 139.83, 131.66, 131.59, 130.86, 130.67, 129.69, 127.55, 127.22, 124.60, 114.92, 55.87; MS (ESI): m/z = 273.2 $(M + H)^+$.

*6.1.1.6 (E)-1-(3-Chlorophenyl)-3-(4-methoxyphenyl)prop-2-en-1-one (**6**).* *p*-Methoxybenzaldehyde and 3′-chloroacetophenone were used as reactants; the resulting precipitate was purified by CC (EtOAc : hexane 2 : 3) followed by washing with diethyl ether (3 × 10 mL) to give the desired pure product as a yellow solid (91% yield); mp 92–94 °C (as reported in ref. 51); ^{1}H NMR (400 MHz, $CDCl_3$) δ 7.86 (s, 1H), 7.76 (d, J = 7.7 Hz, 1H), 7.68 (d, J = 15.6 Hz, 1H), 7.49 (d, J = 8.4 Hz, 2H), 7.42 (d, J = 5.8 Hz, 1H), 7.32 (t, J = 7.8 Hz, 1H), 7.23 (d, J = 15.6 Hz, 1H), 6.83 (d, J = 8.3 Hz, 2H), 3.74 (s, 3H); ^{13}C NMR (101 MHz, $CDCl_3$) δ 188.89, 161.73, 145.33, 139.93, 134.64, 132.24, 130.21, 129.69, 128.29, 127.16, 126.26, 118.90, 114.29, 55.23; MS (ESI): m/z = 273.2 $(M + H)^+$.

*6.1.1.7 (E)-1-(4-Chlorophenyl)-3-(4-methoxyphenyl)prop-2-en-1-one (**7**).* *p*-Methoxybenzaldehyde and 4′-chloroacetophenone were used as reactants; the resulting precipitate was purified by CC (EtOAc : hexane 2 : 3) followed by washing with diethyl ether (3 × 10 mL) to give the desired pure product as a beige solid (82% yield); mp 120–122 °C (as reported in ref. 50); ^{1}H NMR (400 MHz, $CDCl_3$) δ 7.88 (d, J = 8.6 Hz, 2H), 7.72 (d, J = 15.5 Hz, 1H), 7.53 (d, J = 8.9 Hz, 2H), 7.40 (d, J = 8.2 Hz, 2H), 7.29 (d, J = 15.6 Hz, 1H), 6.87 (d, J = 8.8 Hz, 2H), 3.79 (s, 3H); ^{13}C NMR (101 MHz, $CDCl_3$) δ 188.99, 161.67, 145.01, 138.75, 136.63, 130.14, 129.64, 128.68, 127.25, 118.98, 114.29, 55.24; MS (ESI): m/z = 273.1 $(M + H)^+$.

*6.1.1.8 (E)-1-(2-Bromophenyl)-3-(4-methoxyphenyl)prop-2-en-1-one (**8**).* *p*-Methoxybenzaldehyde and 2′-bromoacetophenone were used as reactants; the resulting precipitate was purified by CC (EtOAc : hexane 2 : 3) followed by washing with diethyl ether (3 × 10 mL) to give the desired pure product as a yellow solid (87% yield); mp 89–91 °C (as reported in ref. 52); ^{1}H NMR (400 MHz, $CDCl_3$) δ 7.59 (d, J = 8.0 Hz, 1H), 7.46 (d, J = 8.2 Hz, 2H), 7.36–7.34 (m, 2H), 7.31–7.20 (m, 2H), 6.94–6.84 (m, 3H), 3.79 (s, 3H); ^{13}C NMR (101 MHz, $CDCl_3$) δ 194.94, 162.14, 146.83, 141.55, 133.50, 131.27, 130.56, 129.21, 127.42, 127.23, 124.13, 119.60, 114.62, 55.56; MS (ESI): m/z = 317.1 $(M + H)^+$.

*6.1.1.9 (E)-1-(4-Bromophenyl)-3-(4-methoxyphenyl)prop-2-en-1-one (**9**).* *p*-Methoxybenzaldehyde and 4′-bromoacetophenone were used as reactants; the resulting precipitate was purified by CC (EtOAc : hexane 2 : 3) followed by washing with diethyl ether (3 × 10 mL) to give the desired pure product as a yellowish white solid (86% yield); mp 140–142 °C (as reported in ref. 50); ^{1}H NMR (400 MHz, $CDCl_3$) δ 7.78 (d, J = 8.1 Hz, 2H), 7.69 (d, J = 15.6 Hz, 1H), 7.52 (dd, J = 13.4, 8.3 Hz, 4H), 7.26 (d, J = 15.6 Hz, 1H), 6.85 (d, J = 8.3 Hz, 2H), 3.76 (s, 3H); ^{13}C NMR (101 MHz, $CDCl_3$) δ 189.17, 161.67, 145.07, 137.04, 131.65, 130.15, 129.76, 127.40, 127.23, 118.93, 114.28, 55.24; MS (ESI): m/z = 317.1 $(M + H)^+$.

*6.1.1.10 (E)-1-(2-Hydroxyphenyl)-3-(4-methoxyphenyl)prop-2-en-1-one (**10**).* *p*-Methoxybenzaldehyde and 2′-hydroxyacetophenone were used as reactants; the resulting precipitate was collected by filtration and washed using (3 × 10 mL) of 5 : 3 mixture of methanol and water to give the desired pure product as a yellow solid (83% yield); mp 94–96 °C (as reported in ref. 50); ^{1}H NMR (400 MHz, $CDCl_3$) δ 12.90 (s, 1H), 7.88–7.83 (m, 2H), 7.58 (d, J = 8.3 Hz, 2H), 7.51–7.42 (m, 2H), 6.98 (d, J = 8.4 Hz, 1H), 6.90 (d, J = 8.5 Hz, 3H), 3.82 (s, 3H); ^{13}C NMR (101 MHz, $CDCl_3$) δ 193.66, 163.55, 162.03, 145.35, 136.13, 130.54, 129.53, 127.34, 120.12, 118.74, 118.57, 117.58, 114.52, 55.44; MS (ESI): m/z = 255.2 $(M + H)^+$.

*6.1.1.11 (E)-1-(3-Hydroxyphenyl)-3-(4-methoxyphenyl)prop-2-en-1-one (**11**).* *p*-Methoxybenzaldehyde and 3′-hydroxyacetophenone were used as reactants; the resulting precipitate was collected by filtration and washed using (3 × 10 mL) of 5 : 3 mixture of methanol and water to give the desired pure product as a yellow solid (72% yield); mp 183–185 °C (as reported in ref. 50); ^{1}H NMR (400 MHz, DMSO-d_6) δ 9.78 (s, 1H), 7.82 (d, J = 8.3 Hz, 2H), 7.68 (s, 2H), 7.59 (d, J = 7.6 Hz, 1H), 7.44 (s, 1H), 7.35 (t, J = 7.9 Hz, 1H), 7.02 (dd, J = 18.2, 8.1 Hz, 3H), 3.80 (s, 3H); ^{13}C NMR (101 MHz, DMSO-d_6) δ 188.78, 161.14, 157.50, 143.61, 139.10, 130.54, 129.57, 127.11, 119.85, 119.51, 119.23, 114.36, 114.21, 55.16; MS (ESI): m/z = 255.4 $(M + H)^+$.

*6.1.1.12 (E)-1-(4-Hydroxyphenyl)-3-(4-methoxyphenyl)prop-2-en-1-one (**12**).* *p*-Methoxybenzaldehyde and 4′-hydroxyacetophenone were used as reactants; the resulting precipitate was collected by filtration and washed using (3 × 10 mL) of 5 : 3 mixture of methanol and water to give the desired pure product as a greenish yellow solid (74% yield); mp 187–189 °C (as reported in ref. 50); ^{1}H NMR (400 MHz, DMSO-d_6) δ 10.37 (s, 1H), 8.02 (d, J = 8.2 Hz, 2H), 7.80–7.70 (m, 3H), 7.62 (d, J = 15.5 Hz, 1H), 6.97 (d, J = 8.2 Hz, 2H), 6.87 (d, J = 8.2 Hz, 2H), 3.78 (s, 3H); ^{13}C NMR (101 MHz, DMSO-d_6) δ 187.48, 162.47, 161.53, 143.08, 131.43, 130.95, 129.73, 127.94, 120.02, 115.75, 114.78, 55.76; MS (ESI): m/z = 255.2 $(M + H)^+$.

*6.1.1.13 (E)-1-(4-Ethoxyphenyl)-3-(4-methoxyphenyl)prop-2-en-1-one (**13**).* *p*-Methoxybenzaldehyde and 4′-ethoxyacetophenone were used as reactants; the resulting precipitate was collected by filtration and washed using (3 × 10 mL) of 5 : 3 mixture of methanol and water to give the desired pure product as a white solid (80% yield); mp 112–114 °C (as reported in ref. 50); ^{1}H NMR (400 MHz, $CDCl_3$) δ 7.86 (d, J = 8.4 Hz, 2H), 7.62 (d, J = 15.6 Hz, 1H), 7.44 (d, J = 8.3 Hz, 2H), 7.27 (d, J = 15.5 Hz, 1H), 6.79 (dd, J = 11.5, 8.5 Hz, 4H), 3.95 (q, J = 7.0 Hz, 2H), 3.69 (s, 3H), 1.29 (t, J = 7.0 Hz, 3H); ^{13}C NMR (101 MHz, $CDCl_3$) δ 188.51, 162.50, 161.28, 143.49, 130.96, 130.49, 129.88, 127.64, 119.38, 114.17, 114.01, 63.54, 55.19, 14.49; MS (ESI): m/z = 283.6 $(M + H)^+$.

*6.1.1.14 (E)-3-(4-Methoxyphenyl)-1-(p-tolyl)prop-2-en-1-one (**14**).* *p*-Methoxybenzaldehyde and 1-(*p*-tolyl)ethan-1-one were used as reactants; the resulting precipitate was collected by filtration and washed using (3 × 10 mL) of 5 : 3 mixture of methanol and water to give the desired pure product as a beige solid (75% yield); mp 95–97 °C (as reported in ref. 50); ^{1}H NMR (400 MHz, $CDCl_3$) δ 7.82 (d, J = 7.8 Hz, 2H), 7.67 (d, J = 15.6 Hz, 1H), 7.49 (d, J = 8.8 Hz, 2H), 7.31 (d, J = 14.0 Hz, 1H), 7.19 (d, J = 7.8 Hz, 2H), 6.83 (d, J = 8.8 Hz, 2H), 3.74 (s, 3H), 2.32 (s, 3H); ^{13}C NMR (101 MHz, $CDCl_3$) δ 189.85, 161.39, 144.03, 143.16, 135.72,

129.97, 129.07, 128.37, 127.55, 119.61, 114.20, 55.20, 21.46; MS (ESI): $m/z = 253.5$ $(M + H)^+$.

*6.1.1.15 (E)-1-(2,4-Dichlorophenyl)-3-(4-methoxyphenyl)prop-2-en-1-one (**15**).* *p*-Methoxybenzaldehyde and 2′,4′-dichloroacetophenone were used as reactants;[50] The resulting precipitate was collected by filtration and washed using (3 × 10 mL) of 5 : 3 mixture of methanol and water to give the desired pure product as a yellow semisolid (85% yield); ^{1}H NMR (400 MHz, $CDCl_3$) δ 7.46–7.37 (m, 3H), 7.33 (dd, $J = 12.1$, 3.9 Hz, 2H), 7.25 (dd, $J = 8.2$, 1.9 Hz, 1H), 6.92–6.81 (m, 3H), 3.76 (s, 3H); ^{13}C NMR (101 MHz, $CDCl_3$) δ 193.08, 162.57, 147.08, 138.19, 137.07, 132.72, 130.95, 130.75, 130.57, 127.66, 127.40, 124.16, 114.98, 55.89; MS (ESI): $m/z = 307.1$ $(M + H)^+$.

*6.1.1.16 (E)-1-(3,4-Dichlorophenyl)-3-(4-methoxyphenyl)prop-2-en-1-one (**16**).* *p*-Methoxybenzaldehyde and 3′,4′-dichloroacetophenone were used as reactants; the resulting precipitate was collected by filtration and washed using (3 × 10 mL) of 5 : 3 mixture of methanol and water to give the desired pure product as a yellow solid (75% yield); mp 139–141 °C (as reported in ref. 53); ^{1}H NMR (400 MHz, $CDCl_3$) δ 8.03 (s, 1H), 7.79–7.71 (m, 2H), 7.53 (dd, $J = 14.9$, 8.3 Hz, 3H), 7.26 (d, $J = 15.5$ Hz, 1H), 6.89 (d, $J = 8.3$ Hz, 2H), 3.81 (s, 3H); ^{13}C NMR (101 MHz, $CDCl_3$) δ 188.39, 162.50, 146.37, 138.56, 137.47, 133.64, 131.13, 130.94, 130.83, 127.89, 127.68, 118.98, 114.97, 55.90; MS (ESI): $m/z = 307.2$ $(M + H)^+$.

*6.1.1.17 (E)-1-(2,4-Dichlorophenyl)-3-(3-methoxyphenyl)prop-2-en-1-one (**17**).* *m*-Methoxybenzaldehyde and 2′,4′-dichloroacetophenone were used as reactants; the resulting precipitate was collected by filtration and washed using (3 × 10 mL) of 5 : 3 mixture of methanol and water to give the desired pure product as a white solid (87% yield); mp 95.5–97.5 °C; ^{1}H NMR (400 MHz, $CDCl_3$) δ 7.54–7.18 (m, 5H), 7.18–6.98 (m, 3H), 6.92 (d, $J = 5.9$ Hz, 1H), 3.78 (s, 3H); ^{13}C NMR (101 MHz, $CDCl_3$) δ 192.71, 160.11, 146.63, 137.55, 137.09, 135.74, 132.51, 130.55, 130.35, 130.17, 127.43, 126.29, 121.47, 117.12, 113.51, 55.50; MS (ESI): $m/z = 307.2$ $(M + H)^+$.

*6.1.1.18 (E)-1-(2,4-Dichlorophenyl)-3-(2,4-dimethoxyphenyl) prop-2-en-1-one (**18**).* 2,4-Dimethoxybenzaldehyde and 2′,4′-dichloroacetophenone were used as reactants; the resulting precipitate was collected by filtration and washed with diethyl ether (2 × 6 mL) to give the desired pure product as a white solid (70% yield); mp 108–110 °C (as reported in ref. 54); ^{1}H NMR (400 MHz, $CDCl_3$) δ 7.60 (d, $J = 16.1$ Hz, 1H), 7.41–7.35 (m, 2H), 7.30 (d, $J = 8.1$ Hz, 1H), 7.22 (d, $J = 8.3$ Hz, 1H), 7.00 (d, $J = 16.1$ Hz, 1H), 6.42 (d, $J = 8.7$ Hz, 1H), 6.34 (s, 1H), 3.74 (s, 6H); ^{13}C NMR (101 MHz, $CDCl_3$) δ 193.25, 163.57, 160.43, 142.51, 138.05, 136.28, 132.27, 131.04, 130.30, 130.03, 127.06, 124.12, 116.41, 105.59, 98.39, 55.52, 55.50; MS (ESI): $m/z = 337.1$ $(M + H)^+$.

*6.1.1.19 (E)-1-(2,4-Dichlorophenyl)-3-(2,5-dimethoxyphenyl) prop-2-en-1-one (**19**).* 2,5-Dimethoxybenzaldehyde and 2′,4′-dichloroacetophenone were used as reactants;[55] The resulting precipitate was collected by filtration and washed with diethyl ether (2 × 6 mL) to give the desired pure product as a white solid (73% yield); mp 115–117 °C; ^{1}H NMR (400 MHz, $CDCl_3$) δ 7.64 (d, $J = 16.2$ Hz, 1H), 7.37–7.28 (m, 2H), 7.21 (d, $J = 8.2$ Hz, 1H), 7.06–6.94 (m, 2H), 6.84–6.80 (m, 1H), 6.72 (d, $J = 9.1$ Hz, 1H), 3.69 (s, 3H), 3.66 (s, 3H); ^{13}C NMR (101 MHz, $CDCl_3$) δ 193.04, 153.51, 153.30, 141.89, 137.65, 136.65, 132.36, 130.41, 130.13, 127.16, 126.55, 123.69, 118.18, 113.37, 112.52, 56.07, 55.78; MS (ESI): $m/z = 337.1$ $(M + H)^+$.

*6.1.1.20 (E)-1-(2,4-Dichlorophenyl)-3-(3,4-dimethoxyphenyl) prop-2-en-1-one (**20**).* 3,4-Dimethoxybenzaldehyde and 2′,4′-dichloroacetophenone were used as reactants; the resulting precipitate was collected by filtration and washed with diethyl ether (2 × 6 mL) to give the desired pure product as a white solid (79% yield); mp 132–134 °C (as reported in ref. 56); ^{1}H NMR (400 MHz, $CDCl_3$) δ 7.39 (s, 1H), 7.35–7.25 (m, 3H), 7.06 (d, $J = 6.4$ Hz, 1H), 7.00 (s, 1H), 6.88 (d, $J = 16.0$ Hz, 1H), 6.80 (d, $J = 8.3$ Hz, 1H), 3.84 (s, 6H); ^{13}C NMR (101 MHz, $CDCl_3$) δ 192.64, 151.89, 149.31, 146.94, 137.67, 136.59, 132.23, 130.23, 130.10, 127.20, 127.16, 123.96, 123.57, 111.09, 110.01, 56.00, 55.91; MS (ESI): $m/z = 337.1$ $(M + H)^+$.

*6.1.1.21 (E)-3-(4-Methoxyphenyl)-1-(thiophen-2-yl)prop-2-en-1-one (**21**).* *p*-Methoxybenzaldehyde and 1-(thiophen-2-yl)ethan-1-one were used as reactants; the resulting precipitate was purified by CC (DCM only) followed by washing with diethyl ether (3 × 10 mL) to give the desired pure product as a yellow solid (73% yield); mp 83–85 °C (as reported in ref. 50); ^{1}H NMR (400 MHz, $CDCl_3$) δ 7.71 (d, $J = 16.0$ Hz, 2H), 7.54 (d, $J = 5.0$ Hz, 1H), 7.49 (d, $J = 8.1$ Hz, 2H), 7.19 (d, $J = 15.5$ Hz, 1H), 7.06 (t, $J = 4.4$ Hz, 1H), 6.83 (d, $J = 8.3$ Hz, 2H), 3.74 (s, 3H); ^{13}C NMR (101 MHz, $CDCl_3$) δ 182.04, 161.71, 145.77, 143.86, 133.47, 131.44, 130.26, 128.15, 127.42, 119.27, 114.41, 55.39; MS (ESI): $m/z = 245.2$ $(M + H)^+$.

*6.1.1.22 (E)-3-(4-Methoxyphenyl)-1-(pyridin-2-yl)prop-2-en-1-one (**22**).* *p*-Methoxybenzaldehyde and 1-(pyridin-2-yl)ethan-1-one were used as reactants; the resulting precipitate was purified by CC (DCM only) followed by washing with diethyl ether (3 × 10 mL) to give the desired pure product as a yellow solid (70% yield); mp 80–82 °C (as reported in ref. 50); ^{1}H NMR (400 MHz, $CDCl_3$) δ 8.51 (d, $J = 4.8$ Hz, 1H), 7.99–7.93 (m, 2H), 7.72–7.61 (m, 2H), 7.47 (d, $J = 8.2$ Hz, 2H), 7.27–7.23 (m, 1H), 6.71 (d, $J = 8.2$ Hz, 2H), 3.63 (s, 3H); ^{13}C NMR (101 MHz, $CDCl_3$) δ 189.36, 161.71, 154.45, 148.76, 144.66, 136.94, 130.62, 127.94, 126.68, 122.82, 118.50, 114.30, 55.36; MS (ESI): $m/z = 240.5$ $(M + H)^+$.

*6.1.1.23 (E)-3-(4-Methoxyphenyl)-1-(naphthalen-2-yl)prop-2-en-1-one (**23**).* *p*-Methoxybenzaldehyde and 1-(naphthalen-2-yl) ethan-1-one were used as reactants; the resulting precipitate was purified by CC (DCM only) followed by washing with diethyl ether (3 × 10 mL) to give the desired pure product as a yellow solid (81% yield); mp 91–93 °C (as reported in ref. 51); ^{1}H NMR (400 MHz, $CDCl_3$) δ 8.36 (s, 1H), 7.94 (d, $J = 8.5$ Hz, 1H), 7.83 (d, $J = 7.8$ Hz, 1H), 7.78–7.67 (m, 3H), 7.50–7.39 (m, 5H), 6.79 (d, $J = 8.2$ Hz, 2H), 3.69 (s, 3H); ^{13}C NMR (101 MHz, $CDCl_3$) δ 190.73, 162.13, 145.06, 136.27, 135.83, 133.02, 130.72, 130.15, 129.92, 128.91, 128.68, 128.24, 128.12, 127.15, 124.98, 120.21, 114.87, 55.84; MS (ESI): $m/z = 289.4$ $(M + H)^+$.

*6.1.1.24 (E)-1-([1,1′-Biphenyl]-4-yl)-3-(4-methoxyphenyl)prop-2-en-1-one (**24**).* *p*-Methoxybenzaldehyde and 1-([1,1′-biphenyl]-4-yl)ethan-1-one were used as reactants; the resulting precipitate was purified by CC (DCM only) followed by washing with diethyl ether (3 × 10 mL) to give the desired pure product as a yellow solid (86% yield); mp 88–90 °C (as reported in ref. 50); ^{1}H NMR

(400 MHz, DMSO-d_6) δ 8.21 (d, J = 7.9 Hz, 2H), 7.85–7.70 (m, 8H), 7.51–7.39 (m, 3H), 7.00 (d, J = 8.2 Hz, 2H), 3.80 (s, 3H); ^{13}C NMR (101 MHz, DMSO-d_6) δ 188.04, 160.99, 143.90, 143.57, 138.56, 136.25, 130.44, 128.77, 128.68, 127.94, 126.93, 126.60, 126.51, 119.12, 114.02, 54.97; MS (ESI): m/z = 315.5 $(M + H)^+$.

*6.1.1.25 (E)-3-(4-Methoxyphenyl)-1-(4-phenoxyphenyl)prop-2-en-1-one (**25**).* *p*-Methoxybenzaldehyde and 1-(4-phenoxyphenyl) ethan-1-one were used as reactants; the resulting precipitate was purified by CC (DCM only) followed by washing with diethyl ether (3 × 10 mL) to give the desired pure product as a yellow solid (84% yield); mp 61–63 °C (as reported in ref. 50); ^{1}H NMR (400 MHz, $CDCl_3$) δ 7.91 (d, J = 8.4 Hz, 2H), 7.68 (d, J = 15.5 Hz, 1H), 7.49 (d, J = 8.3 Hz, 2H), 7.33–7.26 (m, 3H), 7.15–7.06 (m, 1H), 6.96 (dd, J = 16.8, 8.1 Hz, 4H), 6.82 (d, J = 8.3 Hz, 2H), 3.74 (s, 3H); ^{13}C NMR (101 MHz, $CDCl_3$) δ 188.86, 161.60, 155.63, 144.25, 133.08, 130.65, 130.15, 130.01, 127.68, 124.48, 120.07, 119.45, 117.45, 114.39, 55.39; MS (ESI): m/z = 331.2 $(M + H)^+$.

*6.1.1.26 (E)-2-(4-Methoxybenzylidene)-2,3-dihydro-1H-inden-1-one (**26**).* *p*-Methoxybenzaldehyde and 2,3-dihydro-1*H*-inden-1-one were used as reactants; the resulting precipitate was collected by filtration and washed using (3 × 10 mL) of 5 : 3 mixture of methanol and water to give the desired pure product as a faint yellow solid (66% yield); mp 120–122 °C (as reported in ref. 50); ^{1}H NMR (400 MHz, $CDCl_3$) δ 7.73 (d, J = 7.6 Hz, 1H), 7.47–7.36 (m, 5H), 7.24 (t, J = 7.3 Hz, 1H), 6.81 (d, J = 8.4 Hz, 2H), 3.82 (s, 2H), 3.69 (s, 3H); ^{13}C NMR (101 MHz, $CDCl_3$) δ 194.33, 160.83, 149.46, 138.22, 134.30, 133.76, 132.53, 132.38, 128.13, 127.54, 126.07, 124.26, 114.44, 55.36, 32.44; MS (ESI): m/z = 251.7 $(M + H)^+$.

*6.1.1.27 (E)-2-(4-Methoxybenzylidene)-3,4-dihydronaphthalen-1(2H)-one (**27**).* *p*-Methoxybenzaldehyde and 3,4-dihydronaphthalen-1(2*H*)-one were used as reactants; the resulting precipitate was collected by filtration and washed using (3 × 10 mL) of 5 : 3 mixture of methanol and water to give the desired pure product as a yellow solid (82% yield); mp 110–112 °C (as reported in ref. 50); ^{1}H NMR (400 MHz, $CDCl_3$) δ 7.99 (d, J = 7.8 Hz, 1H), 7.71 (s, 1H), 7.34–7.27 (m, 3H), 7.22 (t, J = 7.6 Hz, 1H), 7.11 (d, J = 7.5 Hz, 1H), 6.81 (d, J = 8.3 Hz, 2H), 3.71 (s, 3H), 3.02–2.99 (m, 2H), 2.82–2.79 (m, 2H); ^{13}C NMR (101 MHz, $CDCl_3$) δ 188.27, 160.40, 143.50, 137.10, 134.08, 133.97, 133.52, 132.19, 128.83, 128.57, 128.51, 127.40, 114.38, 55.77, 29.22, 27.65; MS (ESI): m/z = 265.2 $(M + H)^+$.

*6.1.1.28 (E)-3-(4-Methoxybenzylidene)chroman-4-one (**28**).* *p*-Methoxybenzaldehyde and chroman-4-one were used as reactants; the resulting precipitate was collected by filtration and washed using (3 × 10 mL) of 5 : 3 mixture of methanol and water to give the desired pure product as a faint yellow solid (85% yield); mp 134–136 °C (as reported in ref. 50); ^{1}H NMR (400 MHz, $CDCl_3$) δ 7.91 (d, J = 9.7 Hz, 1H), 7.73 (s, 1H), 7.36 (t, J = 7.7 Hz, 1H), 7.17 (d, J = 8.3 Hz, 2H), 6.95 (t, J = 7.9 Hz, 1H), 6.86 (d, J = 8.6 Hz, 3H), 5.26 (s, 2H), 3.75 (s, 3H); ^{13}C NMR (101 MHz, $CDCl_3$) δ 182.28, 161.08, 160.84, 137.42, 135.78, 132.18, 129.01, 128.00, 127.13, 122.24, 121.94, 117.93, 114.39, 67.90, 55.52; MS (ESI): m/z = 267.3 $(M + H)^+$.

6.2 Biological evaluation

6.2.1 Human neutrophil isolation. The protocol governing the use of human neutrophils was reviewed and approved by the Institutional Review Board of Chang Gung Memorial Hospital (approval no. 201902217A3) and was conducted in full compliance with the ethical principles outlined in the Declaration of Helsinki. Blood samples were collected from healthy volunteers between 20 and 35 years after obtaining written informed consent. Neutrophils were isolated through a multi-step procedure involving dextran sedimentation, density gradient separation using Ficoll-Hypaque (GE Healthcare, BioTech, Stockholm, Sweden), and subsequent hypotonic lysis of remaining erythrocytes.[57] The resulting neutrophils exhibited viability exceeding 98%, as confirmed by trypan blue exclusion. For the anti-inflammatory assays, the neutrophils were resuspended in Hank's Balanced Salt Solution (HBSS, Gibco, NY, USA) supplemented with 1 mM Ca^{2+} adjusted to a pH of 7.4.[57]

6.2.2 Measurement of superoxide anion release. The generation of SO by activated human neutrophils was assessed by monitoring the reduction of ferricytochrome c. In this procedure, ferricytochrome c (0.6 mg mL^{-1}) was incubated, and neutrophils (6 × 10^5 cells per mL) were treated with either DMSO (0.1%) as a vehicle control or experimental compounds for 5 minutes at 37 °C. The cells were then activated with formyl-L-methionyl-L-leucyl-L-phenylalanine (fMLF, 0.1 μM) in the presence of cytochalasin B (CB, 1 μg mL^{-1}) and incubated for 10 minutes. Changes in absorbance at 550 nm were measured using a Hitachi U-3010 spectrophotometer. LY294002 served as a positive control.[57]

6.2.3 Determination of elastase release. The assay started with the incubation of the elastase substrate, methoxysuccinyl-Ala-Ala-Pro-Val-*p*-nitroanilide (100 μM). Neutrophils (6 × 10^5 cells per mL) were preincubated with DMSO (0.1%) or experimental compounds for 5 minutes at 37 °C, followed by stimulation with fMLF (0.1 μM) in the presence of cytochalasin B (0.5 μg mL^{-1}). The elastase-mediated cleavage of the substrate was monitored by recording the absorbance at 405 nm using a Hitachi U-3010 spectrophotometer. LY294002 was utilized as a positive control.[57]

6.2.4 Cytotoxicity assay. Cell viability was evaluated by measuring lactate dehydrogenase (LDH) release using a commercially available kit (Promega, Madison, WI, USA). Neutrophils (6 × 10^5 cells per mL) were treated with either DMSO (0.1%) or test compounds (10 μM) for 15 minutes at 37 °C. To determine total LDH activity, cells were lysed with 0.1% Triton X-100 for 30 minutes at 37 °C. The resulting supernatant was collected by centrifugation, subjected to LDH detection reagent, and the change in absorbance was measured at 490 nm using a Hitachi U-3010 spectrophotometer.[35]

6.2.5 Measurement of intracellular Ca^{2+} mobilization. Neutrophils were incubated with 5 μM of Fluo-4 acetoxymethyl ester (Fluo-4/AM, purchased from Invitrogen, OR, USA) at 37 °C for 30 min. Fluo-4-labeled human neutrophils were treated with DMSO (0.1%, as control) or compound **17** at 37 °C for 5 min, and then the increase of intracellular calcium concentration ($[Ca^{2+}]_i$) was obtained by adding fMLF (0.1 μM). The $[Ca^{2+}]_i$ was determined by the fluorescence changes (excitation 494 nm and emission 516 nm) using a spectrofluorometer (Hitachi F 4500; Tokyo, Japan).[35]

6.2.6 Analysis of neutrophil migration. A micro-chemotaxis chamber with 3-μm pore size was used to test neutrophil

migration. DMSO (0.1%, as control) or compound **17**-pretreated neutrophils were placed in the upper chamber, and then the upper chambers were placed into the bottom wells with or without fMLF (0.1 μM) as chemoattractant. The number of migrated cells in bottom wells was detected using Accuri C6 flow cytometer (BD Biosciences, CA, USA).

6.2.7 Immunoblotting assay. Immunoblot analyses were performed following the procedures outlined in ref. 29. The primary antibodies used targeted total and phosphorylated forms of p38 (1 : 8000), JNK (1 : 3000), Akt (1 : 5000), ERK (1 : 8000) along with paxillin, phospho-paxillin (Y31 and Y118), FAK, and phospho-FAK (Y397, Y576/577, and Y925). Proteins were detected using HRP-conjugated anti-rabbit IgG, and immunoreactive bands were visualized *via* chemiluminescence and quantified using a ChemiDoc MP Imaging System (Bio-Rad, USA).[35]

6.2.8 Statistics. Data were analyzed using GraphPad Prism software (version 9.0, GraphPad Software, San Diego, CA, USA). All results are presented as the mean ± standard error of the mean (SEM). Statistical significance was evaluated using Student's test, with $p < 0.05$ defined as the threshold for significance.

Author contributions

All authors: writing – review & editing, writing – original draft. D. S. E.: methodology, investigation, data curation. M. A. H.: methodology, investigation. M. E.: methodology, investigation. D. E. H.: methodology, investigation. M. E.: methodology, investigation. Y.-C. C.: methodology, investigation. Y.-H. W.: methodology, investigation. P.-H. K.: methodology, investigation. M. K.: methodology, investigation. M. A.-H.: supervision, project administration, methodology, investigation, conceptualization, data curation. T.-L. H.: supervision, project administration, methodology, investigation, conceptualization, funding.

Conflicts of interest

The authors declare no conflict of interest.

Data availability

The data supporting the conclusions of this work can be provided by the corresponding authors (MA-H and T-LH) upon reasonable inquiry.

Supplementary information (SI): ^{1}H and ^{13}C NMR, mass spectra, and UHPLC chromatograms of all candidates are provided (Fig. S1–S112). See DOI: https://doi.org/10.1039/d6ra01300g.

Acknowledgements

This research was supported by grants from the Chang Gung University of Science and Technology (ZRRPF3L0091 and ZRRPF3N0101) and Chang Gung Memorial Hospital (CMRPF1M0101-2, CMRPF1M0131-2, CMRPF1N0021, CORPF1N0071-3, CORPF1N0091-3, and BMRP450), Taiwan.

References

1 C. Rosales, Neutrophil: A Cell with Many Roles in Inflammation or Several Cell Types?, *Front. Physiol.*, 2018, **9**, 113, DOI: 10.3389/fphys.2018.00113.
2 V. Witko-Sarsat, P. Rieu, B. Descamps-Latscha, P. Lesavre and L. Halbwachs-Mecarelli, Neutrophils: molecules, functions and pathophysiological aspects, *Lab. Invest.*, 2000, **80**(5), 617–653, DOI: 10.1038/labinvest.3780067.
3 E. Kolaczkowska and P. Kubes, Neutrophil recruitment and function in health and inflammation, *Nat. Rev. Immunol.*, 2013, **13**(3), 159–175, DOI: 10.1038/nri3399.
4 A. Kasorn, P. Alcaide, Y. Jia, K. K. Subramanian, B. Sarraj, Y. Li, F. Loison, H. Hattori, L. E. Silberstein, W. F. Luscinskas, *et al.*, Focal adhesion kinase regulates pathogen-killing capability and life span of neutrophils via mediating both adhesion-dependent and -independent cellular signals, *J. Immunol.*, 2009, **183**(2), 1032–1043, DOI: 10.4049/jimmunol.0802984.
5 A. M. Lopez-Colome, I. Lee-Rivera, R. Benavides-Hidalgo and E. Lopez, Paxillin: a crossroad in pathological cell migration, *J. Hematol. Oncol.*, 2017, **10**(1), 50, DOI: 10.1186/s13045-017-0418-y.
6 M. Bachmann, A. Skripka, K. Weissenbruch, B. Wehrle-Haller and M. Bastmeyer, Phosphorylated paxillin and phosphorylated FAK constitute subregions within focal adhesions, *J. Cell Sci.*, 2022, **135**(7), jcs258764, DOI: 10.1242/jcs.258764.
7 Y. Le, Y. Yang, Y. Cui, H. Yazawa, W. Gong, C. Qiu and J. M. Wang, Receptors for chemotactic formyl peptides as pharmacological targets, *Int. Immunopharmacol.*, 2002, **2**(1), 1–13, DOI: 10.1016/s1567-5769(01)00150-3.
8 H. R. Liao, C. R. Chien, J. J. Chen, T. Y. Lee, S. Z. Lin and C. P. Tseng, The anti-inflammatory effect of 2-(4-hydroxy-3-prop-2-enyl-phenyl)-4-prop-2-enyl-phenol by targeting Lyn kinase in human neutrophils, *Chem.-Biol. Interact.*, 2015, **236**, 90–101, DOI: 10.1016/j.cbi.2015.05.004.
9 J. Hann, J. L. Bueb, F. Tolle and S. Brechard, Calcium signaling and regulation of neutrophil functions: Still a long way to go, *J. Leukocyte Biol.*, 2020, **107**(2), 285–297, DOI: 10.1002/JLB.3RU0719-241R.
10 D. Kim and C. L. Haynes, The role of p38 MAPK in neutrophil functions: single cell chemotaxis and surface marker expression, *Analyst*, 2013, **138**(22), 6826–6833, DOI: 10.1039/c3an01076g.
11 U. Moens, S. Kostenko and B. Sveinbjornsson, The Role of Mitogen-Activated Protein Kinase-Activated Protein Kinases (MAPKAPKs) in Inflammation, *Genes*, 2013, **4**(2), 101–133, DOI: 10.3390/genes4020101.
12 R. M. Lucas, L. Luo and J. L. Stow, ERK1/2 in immune signalling, *Biochem. Soc. Trans.*, 2022, **50**(5), 1341–1352, DOI: 10.1042/BST20220271.
13 J. P. Hall, E. Merithew and R. J. Davis, c-Jun N-terminal kinase (JNK) repression during the inflammatory

response? Just say NO, *Proc. Natl. Acad. Sci. U. S. A.*, 2000, **97**(26), 14022–14024, DOI: 10.1073/pnas.97.26.14022.

14 P. T. Hawkins and L. R. Stephens, PI3K signalling in inflammation, *Biochim. Biophys. Acta*, 2015, **1851**(6), 882–897, DOI: 10.1016/j.bbalip.2014.12.006.

15 K. D. Puri, T. A. Doggett, C. Y. Huang, J. Douangpanya, J. S. Hayflick, M. Turner, J. Penninger and T. G. Diacovo, The role of endothelial PI3Kgamma activity in neutrophil trafficking, *Blood*, 2005, **106**(1), 150–157, DOI: 10.1182/blood-2005-01-0023.

16 T. J. Moraes and G. P. Downey, Neutrophil cell signaling in infection: role of phosphatidylinositide 3-kinase, *Microbes Infect.*, 2003, **5**(14), 1293–1298, DOI: 10.1016/j.micinf.2003.09.012.

17 S. C. Yang, Y. H. Wang, Y. F. Tsai, Y. W. Chang, T. S. Wu, C. M. Ho and T. L. Hwang, A synthesized heterocyclic chalcone inhibits neutrophilic inflammation through K(+)-dependent pH regulation, *FASEB J.*, 2020, **34**(5), 7127–7143, DOI: 10.1096/fj.201903123R.

18 B. Amulic, C. Cazalet, G. L. Hayes, K. D. Metzler and A. Zychlinsky, Neutrophil function: from mechanisms to disease, *Annu. Rev. Immunol.*, 2012, **30**, 459–489, DOI: 10.1146/annurev-immunol-020711-074942.

19 A. Herrero-Cervera, O. Soehnlein and E. Kenne, Neutrophils in chronic inflammatory diseases, *Cell. Mol. Immunol.*, 2022, **19**(2), 177–191, DOI: 10.1038/s41423-021-00832-3.

20 P. Singh, A. Anand and V. Kumar, Recent developments in biological activities of chalcones: a mini review, *Eur. J. Med. Chem.*, 2014, **85**, 758–777, DOI: 10.1016/j.ejmech.2014.08.033.

21 N. A. A. Elkanzi, H. Hrichi, R. A. Alolayan, W. Derafa, F. M. Zahou and R. B. Bakr, Synthesis of Chalcones Derivatives and Their Biological Activities: A Review, *ACS Omega*, 2022, **7**(32), 27769–27786, DOI: 10.1021/acsomega.2c01779.

22 J. S. Lee, S. N. Bukhari and N. M. Fauzi, Effects of chalcone derivatives on players of the immune system, *Drug Des., Dev. Ther.*, 2015, **9**, 4761–4778, DOI: 10.2147/DDDT.S86242.

23 H. H. Ko, L. T. Tsao, K. L. Yu, C. T. Liu, J. P. Wang and C. N. Lin, Structure-activity relationship studies on chalcone derivatives. the potent inhibition of chemical mediators release, *Bioorg. Med. Chem.*, 2003, **11**(1), 105–111, DOI: 10.1016/s0968-0896(02)00312-7.

24 H. S. Ban, K. Suzuki, S. S. Lim, S. H. Jung, S. Lee, J. Ji, H. S. Lee, Y. S. Lee, K. H. Shin and K. Ohuchi, Inhibition of lipopolysaccharide-induced expression of inducible nitric oxide synthase and tumor necrosis factor-alpha by 2'-hydroxychalcone derivatives in RAW 264.7 cells, *Biochem. Pharmacol.*, 2004, **67**(8), 1549–1557, DOI: 10.1016/j.bcp.2003.12.016.

25 S. N. Bukhari, Y. Tajuddin, V. J. Benedict, K. W. Lam, I. Jantan, J. Jalil and M. Jasamai, Synthesis and evaluation of chalcone derivatives as inhibitors of neutrophils' chemotaxis, phagocytosis and production of reactive oxygen species, *Chem. Biol. Drug Des.*, 2014, **83**(2), 198–206, DOI: 10.1111/cbdd.12226.

26 F. Herencia, M. L. Ferrandiz, A. Ubeda, J. N. Dominguez, J. E. Charris, G. M. Lobo and M. J. Alcaraz, Synthesis and anti-inflammatory activity of chalcone derivatives, *Bioorg. Med. Chem. Lett.*, 1998, **8**(10), 1169–1174, DOI: 10.1016/s0960-894x(98)00179-6.

27 T. L. Hwang, S. H. Yeh, Y. L. Leu, C. Y. Chern and H. C. Hsu, Inhibition of superoxide anion and elastase release in human neutrophils by 3'-isopropoxychalcone via a cAMP-dependent pathway, *Br. J. Pharmacol.*, 2006, **148**(1), 78–87, DOI: 10.1038/sj.bjp.0706712.

28 Y. C. Wu, M. Sureshbabu, Y. C. Fang, Y. H. Wu, Y. H. Lan, F. R. Chang, Y. W. Chang and T. L. Hwang, Potent inhibition of human neutrophil activations by bractelactone, a novel chalcone from Fissistigma bracteolatum, *Toxicol. Appl. Pharmacol.*, 2013, **266**(3), 399–407, DOI: 10.1016/j.taap.2012.11.021.

29 M. Abdel-Halim, D. S. El-Gamil, M. A. Hammam, M. El-Shazly, Y. H. Wang, P. H. Kung, Y. C. Chen, M. Korinek, A. H. Abadi, M. Engel, *et al.*, Discovery of 1,3-disubstituted prop-2-en-1-one derivatives as inhibitors of neutrophilic inflammation via modulation of MAPK and Akt pathways, *J. Enzyme Inhib. Med. Chem.*, 2024, **39**(1), 2402988, DOI: 10.1080/14756366.2024.2402988.

30 P. J. Honeycutt and J. E. Niedel, Cytochalasin B enhancement of the diacylglycerol response in formyl peptide-stimulated neutrophils, *J. Biol. Chem.*, 1986, **261**(34), 15900–15905.

31 H. Fu, L. Bjorkman, P. Janmey, A. Karlsson, J. Karlsson, C. Movitz and C. Dahlgren, The two neutrophil members of the formylpeptide receptor family activate the NADPH-oxidase through signals that differ in sensitivity to a gelsolin derived phosphoinositide-binding peptide, *BMC Cell Biol.*, 2004, **5**(1), 50, DOI: 10.1186/1471-2121-5-50.

32 D. Mulugeta, A Review of Synthesis Methods of Chalcones, Flavonoids, and Coumarins, *Sci. J. Chem.*, 2022, **10**(2), 41–52, DOI: 10.11648/j.sjc.20221002.12.

33 T. P. Setyaningrum, E. M. Sitompul, Z. Zulhipri, F. Kurniadewi and H. Dianhar, Development of chalcone synthesis: Optimization of synthetic method, in *AIP Conf. Proc.*, 2023, vol. 2913, p 020001.

34 P. Kumar, A. Nagarajan and P. D. Uchil, Analysis of Cell Viability by the Lactate Dehydrogenase Assay, *Cold Spring Harb. Protoc.*, 2018, **2018**(6), 465–468, DOI: 10.1101/pdb.prot095497.

35 M. Abdel-Halim, R. A. Wagdy, M. Salah, Y. H. Wang, T. P. Cheng, Y. R. Lee, Y. C. Chen, Y. M. Mandour, A. H. Abadi, M. Engel, *et al.*, Targeting Neutrophil-Mediated Inflammation: Identification of Pyrazolidinone Carboxamide Derivatives as Potent Selective Inhibitors of Formyl Peptide Receptor 1 (FPR1)-Activated Neutrophils, *ACS Pharmacol. Transl. Sci.*, 2025, **8**(6), 1591–1609, DOI: 10.1021/acsptsci.4c00715.

36 K. Aoshiba, S. Yasui, M. Hayashi, J. Tamaoki and A. Nagai, Role of p38-Mitogen-Activated Protein Kinase in Spontaneous Apoptosis of Human Neutrophils, *J. Immunol.*, 1999, **162**(3), 1692–1700, DOI: 10.4049/jimmunol.162.3.1692.

37 N. Hu, Y. Qiu and F. Dong, Role of Erk1/2 signaling in the regulation of neutrophil versus monocyte development in response to G-CSF and M-CSF, *J. Biol. Chem.*, 2015, **290**(40), 24561–24573, DOI: 10.1074/jbc.M115.668871.

38 F. A. Simard, A. Cloutier, T. Ear, H. Vardhan and P. P. McDonald, MEK-independent ERK activation in human neutrophils and its impact on functional responses, *J. Leukocyte Biol.*, 2015, **98**(4), 565–573, DOI: 10.1189/jlb.2MA1214-599R.

39 M. A. Khan, A. Farahvash, D. N. Douda, J. C. Licht, H. Grasemann, N. Sweezey and N. Palaniyar, JNK Activation Turns on LPS- and Gram-Negative Bacteria-Induced NADPH Oxidase-Dependent Suicidal NETosis, *Sci. Rep.*, 2017, **7**(1), 3409, DOI: 10.1038/s41598-017-03257-z.

40 M. L. B. Gronloh, J. J. G. Arts, E. K. Mahlandt, M. A. Nolte, J. Goedhart and J. D. van Buul, Primary adhered neutrophils increase JNK1-MARCKSL1-mediated filopodia to promote secondary neutrophil transmigration, *iScience*, 2023, **26**(8), 107406, DOI: 10.1016/j.isci.2023.107406.

41 T. S. Panetti, Tyrosine phosphorylation of paxillin, FAK, and p130CAS: effects on cell spreading and migration, *Front. Biosci.*, 2002, **7**, d143–d150, DOI: 10.2741/A771.

42 S. A. Parsons, R. Sharma, D. L. Roccamatisi, H. Zhang, B. Petri, P. Kubes, P. Colarusso and K. D. Patel, Endothelial paxillin and focal adhesion kinase (FAK) play a critical role in neutrophil transmigration, *Eur. J. Immunol.*, 2012, **42**(2), 436–446, DOI: 10.1002/eji.201041303.

43 J. O. Abaricia, A. H. Shah and R. Olivares-Navarrete, Substrate stiffness induces neutrophil extracellular trap (NET) formation through focal adhesion kinase activation, *Biomaterials*, 2021, **271**, 120715, DOI: 10.1016/j.biomaterials.2021.120715.

44 R. Wang, R. Li, H. Yang, X. Chen, L. Wu, X. Zheng and Y. Jin, Flavokawain C inhibits proliferation and migration of liver cancer cells through FAK/PI3K/AKT signaling pathway, *J. Cancer Res. Clin. Oncol.*, 2024, **150**(3), 117, DOI: 10.1007/s00432-024-05639-z.

45 S. H. Lin and Y. W. Shih, Antitumor effects of the flavone chalcone: inhibition of invasion and migration through the FAK/JNK signaling pathway in human gastric adenocarcinoma AGS cells, *Mol. Cell. Biochem.*, 2014, **391**(1–2), 47–58, DOI: 10.1007/s11010-014-1986-6.

46 R. Immler, S. I. Simon and M. Sperandio, Calcium signalling and related ion channels in neutrophil recruitment and function, *Eur. J. Clin. Invest.*, 2018, **48**(Suppl 2), e12964, DOI: 10.1111/eci.12964.

47 P. Nordenfelt and H. Tapper, The role of calcium in neutrophil granule-phagosome fusion, *Commun. Integr. Biol.*, 2010, **3**(3), 224–226, DOI: 10.4161/cib.3.3.11168.

48 A. K. Gupta, S. Giaglis, P. Hasler and S. Hahn, Efficient neutrophil extracellular trap induction requires mobilization of both intracellular and extracellular calcium pools and is modulated by cyclosporine A, *PLoS One*, 2014, **9**(5), e97088, DOI: 10.1371/journal.pone.0097088.

49 M. Abdel-Halim, A. H. Abadi and M. Engel, Design and synthesis of novel 1,3,5-triphenyl pyrazolines as potential anti-inflammatory agents through allosteric inhibition of protein kinase Czeta (PKCzeta), *Medchemcomm*, 2018, **9**(6), 1076–1082, DOI: 10.1039/c8md00100f.

50 M. Abdel-Halim, S. Sigler, N. A. S. Racheed, A. Hefnawy, R. K. Fathalla, M. A. Hammam, A. Maher, Y. Maxuitenko, A. B. Keeton, R. W. Hartmann, *et al.*, From Celecoxib to a Novel Class of Phosphodiesterase 5 Inhibitors: Trisubstituted Pyrazolines as Novel Phosphodiesterase 5 Inhibitors with Extremely High Potency and Phosphodiesterase Isozyme Selectivity, *J. Med. Chem.*, 2021, **64**(8), 4462–4477, DOI: 10.1021/acs.jmedchem.0c01120.

51 F. Zhao, Q.-J. Zhao, J.-X. Zhao, D.-Z. Zhang, Q.-Y. Wu and Y.-S. Jin, Synthesis and cdc25B inhibitory activity evaluation of chalcones, *Chem. Nat. Compd.*, 2013, **49**(2), 206–214.

52 X.-D. Fei, Z. Zhou, W. Li, Y.-M. Zhu and J.-K. Shen, Buchwald-Hartwig Coupling/Michael Addition Reactions: One-Pot Synthesis of 1,2-Disubstituted 4-Quinolones from Chalcones and Primary Amines, *Eur. J. Org Chem.*, 2012, **2012**(15), 3001–3008.

53 Y. Zheng, X. Wang, S. Gao, M. Ma, G. Ren, H. Liu and X. Chen, Synthesis and antifungal activity of chalcone derivatives, *Nat. Prod. Res.*, 2015, **29**(19), 1804–1810.

54 R. Li, G. L. Kenyon, F. E. Cohen, X. Chen, B. Gong, J. N. Dominguez, E. Davidson, G. Kurzban, R. E. Miller, E. O. Nuzum, *et al.*, In vitro antimalarial activity of chalcones and their derivatives, *J. Med. Chem.*, 1995, **38**(26), 5031–5037, DOI: 10.1021/jm00026a010.

55 N. K. Sahu, S. B. Bari and D. V. Kohli, QSAR Studies of Some Substituted 1,3-Diaryl Propenone Derivatives as Plasmodium falciparum Growth Inhibitors, *Lett. Drug Des. Discovery*, 2012, **9**(2), 153–162, DOI: 10.2174/157018012799079644.

56 T. Narender and K. Papi Reddy, A simple and highly efficient method for the synthesis of chalcones by using borontrifluoride-etherate, *Tetrahedron Lett.*, 2007, **48**(18), 3177–3180.

57 N. B. A. Nguyen, L. Y. Chen, P. J. Chen, M. El-Shazly, T. L. Hwang, J. H. Su, C. H. Su, P. T. Yen, B. R. Peng and K. H. Lai, MS/MS Molecular Networking Unveils the Chemical Diversity of Biscembranoid Derivatives, Neutrophilic Inflammatory Mediators from the Cultured Soft Coral Sarcophyton trocheliophorum, *Int. J. Mol. Sci.*, 2022, **23**(24), 15464, DOI: 10.3390/ijms232415464.